



**Environmental Security Technology Certification Program  
(ESTCP)**

**Final Report**

**Demonstration of Airborne Wide Area Assessment Technologies at  
Kirtland Precision Bombing Range, New Mexico**



**Project No. 200535: Innovative Multi-Sensor Airborne Wide Area  
Assessment of UXO Sites**

**April 2008  
Version 2.1**

**REPORT DOCUMENTATION PAGE**

*Form Approved  
OMB No. 0704-0188*

The public reporting burden for this collection of information is estimated to average 1 hour per response, including the time for reviewing instructions, searching existing data sources, gathering and maintaining the data needed, and completing and reviewing the collection of information. Send comments regarding this burden estimate or any other aspect of this collection of information, including suggestions for reducing the burden, to the Department of Defense, Executive Services and Communications Directorate (0704-0188). Respondents should be aware that notwithstanding any other provision of law, no person shall be subject to any penalty for failing to comply with a collection of information if it does not display a currently valid OMB control number.

**PLEASE DO NOT RETURN YOUR FORM TO THE ABOVE ORGANIZATION.**

<b>1. REPORT DATE (DD-MM-YYYY)</b>		<b>2. REPORT TYPE</b>		<b>3. DATES COVERED (From - To)</b>	
<b>4. TITLE AND SUBTITLE</b>				<b>5a. CONTRACT NUMBER</b>	
				<b>5b. GRANT NUMBER</b>	
				<b>5c. PROGRAM ELEMENT NUMBER</b>	
<b>6. AUTHOR(S)</b>				<b>5d. PROJECT NUMBER</b>	
				<b>5e. TASK NUMBER</b>	
				<b>5f. WORK UNIT NUMBER</b>	
<b>7. PERFORMING ORGANIZATION NAME(S) AND ADDRESS(ES)</b>				<b>8. PERFORMING ORGANIZATION REPORT NUMBER</b>	
<b>9. SPONSORING/MONITORING AGENCY NAME(S) AND ADDRESS(ES)</b>				<b>10. SPONSOR/MONITOR'S ACRONYM(S)</b>	
				<b>11. SPONSOR/MONITOR'S REPORT NUMBER(S)</b>	
<b>12. DISTRIBUTION/AVAILABILITY STATEMENT</b>					
<b>13. SUPPLEMENTARY NOTES</b>					
<b>14. ABSTRACT</b>					
<b>15. SUBJECT TERMS</b>					
<b>16. SECURITY CLASSIFICATION OF:</b>			<b>17. LIMITATION OF ABSTRACT</b>	<b>18. NUMBER OF PAGES</b>	<b>19a. NAME OF RESPONSIBLE PERSON</b>
<b>a. REPORT</b>	<b>b. ABSTRACT</b>	<b>c. THIS PAGE</b>			<b>19b. TELEPHONE NUMBER (Include area code)</b>

## TABLE OF CONTENTS

<b>REPORT DOCUMENTATION</b> .....	i
<b>TABLE OF CONTENTS</b> .....	ii
<b>ACRONYMS</b> .....	vi
<b>ACKNOWLEDGMENTS</b> .....	vii
<b>1. INTRODUCTION</b> .....	1
1.1. Background .....	1
1.2. Objectives of the Demonstration .....	1
1.3. Regulatory Drivers .....	2
1.4. Stakeholder/End-User Issues .....	2
<b>2. TECHNOLOGY DESCRIPTION</b> .....	3
2.1. Technology Development and Application .....	3
2.1.1. Helicopter Platform .....	3
2.1.2. Sensors and Boom .....	4
2.1.3. Positioning Technologies .....	5
2.1.4. Data Acquisition System .....	5
2.1.5. Data Processing .....	5
2.1.6. Data Analysis .....	6
2.2. Previous Testing of the Technology .....	7
2.3. Factors Affecting Cost and Performance .....	7
2.4. Advantages and Limitations of the Technology .....	7
<b>3. DEMONSTRATION DESIGN</b> .....	8
3.1. Performance Objectives .....	8
3.2. Test Site Selection .....	8
3.3. Test Site History/Characteristics .....	8
3.4. Present Operations .....	13
3.5. Pre-Demonstration Testing and Analysis .....	14
3.6. Testing and Evaluation Plan .....	14
3.6.1. Demonstration Set-Up and Start-Up .....	14
3.6.2. Period of Operation .....	15
3.6.3. Area Characterized .....	16
3.6.4. Operating Parameters for the Technology .....	16
3.6.5. Data Processing .....	17
3.6.6. Data Analysis .....	20
3.6.7. Demobilization .....	23
<b>4. PERFORMANCE ASSESSMENT</b> .....	24
4.1. Data Calibration Results .....	24
4.1.1. Data Calibration .....	24
4.1.2. Calibration Item Response .....	24
4.2. Overall Results .....	27
4.2.1. Anomaly Picking Results .....	27

4.2.2.	Metal Density Analysis.....	28
4.2.3.	Target Dipole-Fit Analyses.....	31
4.2.4.	Intrusive Investigation Results.....	31
4.3.	Results Discussion by Area .....	33
4.3.1.	Target N-2 Area .....	33
4.3.2.	Target N-3 Area .....	33
4.3.3.	SORT Area.....	35
4.3.4.	NDIA Area.....	37
4.3.5.	Possible Areas of Interest.....	39
4.3.6.	Center Fence Line Area .....	42
4.3.7.	Roadbed Alignment Area .....	43
4.4.	Performance Criteria.....	43
4.5.	Performance Confirmation Methods.....	44
<b>5.</b>	<b>COST ASSESSMENT.....</b>	<b>46</b>
5.1.	Cost Reporting .....	46
5.2.	Cost Analysis .....	46
<b>6.</b>	<b>IMPLEMENTATION ISSUES.....</b>	<b>48</b>
6.1.	Regulatory and End-User Issues.....	48
<b>7.</b>	<b>REFERENCES.....</b>	<b>49</b>
<b>8.</b>	<b>POINTS OF CONTACT .....</b>	<b>50</b>

## LIST OF FIGURES

<b>Figure 1.</b>	Helicopter MTADS technology as deployed on Bell Long Ranger helicopter at former KPBR. ....	4
<b>Figure 2.</b>	The track guidance system provides flight traverse information to the pilot. ....	4
<b>Figure 3.</b>	Helicopter MTADS processing flow chart.....	6
<b>Figure 4.</b>	WAA demonstration area and helicopter survey boundaries for October 2005 HeliMag survey at the former KPBR.....	10
<b>Figure 5.</b>	Three additional areas were surveyed in February 2007 shown with approximate boundaries shown in red, green and blue.....	11
<b>Figure 6.</b>	Utilities infrastructure present at the former KPBR. ....	13
<b>Figure 7.</b>	Map of as-flown HeliMag survey altitudes at former KPBR, 2005 and 2007. ....	17
<b>Figure 8.</b>	Total magnetic field grid image of the sample area used to calibrate the automatic target picking routine. ....	21
<b>Figure 9.</b>	Total number of selected targets as a function of cut-off threshold amplitude. ....	22

**Figure 10.** Number of targets automatically selected, normalized by the number of targets manually selected, as a function of cut-off threshold amplitude. .... 22

**Figure 11.** Derived positions for each target relative to the ground truth supplied. .... 25

**Figure 12.** Dipole fit depth estimates for calibration line targets..... 25

**Figure 13.** Dipole fit size estimates for calibration line targets. .... 26

**Figure 14.** Dipole fit solid angle estimate for calibration line targets..... 26

**Figure 15.** Peak analytic signal response for the calibration line targets after upward continuation of the magnetometer data to simulate 0.75 m burial of targets..... 27

**Figure 16.** Geophysical anomalies shown overlain north and south study area on the total field geophysical data..... 29

**Figure 17.** HeliMag anomaly density across all areas surveyed at the former KPBR. .... 30

**Figure 18.** Intrusive investigation results for all selected anomalies. These results are an aggregate of the results from each area selected for intrusive investigation. .... 32

**Figure 19.** HeliMag target density and anomalies in the N-2 target area identified in the CSM. 33

**Figure 20.** HeliMag target density and anomalies in the N-3 target area identified in the CSM. 34

**Figure 21.** Intrusive investigation results for the N-3 area. .... 34

**Figure 22.** Depth distribution for targets investigated at the N-3 impact site..... 35

**Figure 23.** HeliMag target density and anomalies in the SORT area identified in the CSM..... 36

**Figure 24.** Intrusive results for the SORT area. .... 36

**Figure 25.** Depth distribution for targets investigated at the N-3 impact site..... 37

**Figure 26.** HeliMag target density and anomalies in the NDIA area identified in the CSM. .... 38

**Figure 27.** Intrusive results for the NDIA area. .... 38

**Figure 28.** Predicted and observed depths for selected target in the NDIA area. .... 39

**Figure 29.** Possible areas of interest located in west region of the north study area. These elevated anomaly densities appear to be associated with a region of elevated geologic response. .... 40

**Figure 30.** Possible areas of interest located in the northern area of the study area. Areas outlined in light blue appear to be associated with regions of elevated geologic response. Additional intrusive investigations were performed in the AOI North area. .... 40

**Figure 31.** Possible area of interest located in NW region of the south study area. Areas outlined in light blue appear to be associated with regions of elevated geologic response. Additional intrusive investigations were performed in the AOI South area. .... 41

**Figure 32.** Intrusive investigation results for AOI- North and AOI-South..... 41

**Figure 33.** HeliMag targets and target density for the fence line area surveyed in 2007. .... 42

**Figure 34.** HeliMag targets and target density in the Paseo Del Volcan roadway alignment area surveyed in 2007. .... 43

## **LIST OF TABLES**

<b>Table 1.</b> Sky Research HeliMag Technology Components .....	3
<b>Table 2.</b> Performance Objectives .....	9
<b>Table 3.</b> Calibration Items Seeded in the Calibration Lane .....	15
<b>Table 4.</b> HeliMag Data Collection Acreage, 2005 .....	16
<b>Table 5.</b> Helicopter MTADS Raw Data Input Files .....	18
<b>Table 6.</b> Calibration Results for Calibration Lane Targets .....	24
<b>Table 7.</b> Dig Results Comparison for HeliMag and Vehicular Towed System .....	31
<b>Table 8.</b> Performance Criteria for the Former KPBR HeliMag Technology Demonstration .....	44
<b>Table 9.</b> Performance Metrics Confirmation Methods and Results .....	45
<b>Table 10.</b> Cost Tracking .....	47
<b>Table 11.</b> Points of Contact .....	50

## ACRONYMS

AGL	Above Ground Level
ASR	Archive Search Report
CRADA	Cooperative Research and Development Agreement
Cs	Cesium
CSM	Conceptual Site Model
DAQ	Data Acquisition Computer
DEM	Digital Elevation Model
DERP	Defense Environmental Restoration Program
DGM	Digital Geophysical Mapping
DoD	Department of Defense
DSB	Defense Science Board
ESTCP	Environmental Security Technology Certification Program
ft	feet
FUDS	Formerly Used Defense Sites
GIS	Geographic Information Systems
GPS	Global Positioning System
HE	High Explosive
HeliMag	Helicopter MTADS Magnetometry (see MTADS)
Hz	hertz
IMU	Inertial Measurement Unit
KPBR	Kirtland Precision Bombing Range
lb	pound
LiDAR	Light Detection and Ranging
m	meter(s)
m/s	meter(s) per second
MEC	Munitions and Explosives of Concern
MTADS	Multi-sensor Towed Array Detection System
NDIA	New Demolition Impact Area
NRL	Naval Research Laboratory
nT	nanotesla
OB/OD	Open Burn/Open Detonation
PPS	Pulse per second
RTK GPS	Real-Time Kinematic Global Positioning System
SORT	Simulated Oil Refinery Target
TOA	Time of Applicability
UTC	Universal Time Coordinated
UTM	Universal Transverse Mercator
UXO	Unexploded Ordnance
WAA	Wide Area Assessment
WAA-PP	Wide Area Assessment-Pilot Program

## **ACKNOWLEDGMENTS**

*Demonstration of Airborne Wide Area Assessment Technologies at Kirtland Precision Bombing Range, New Mexico* documents the acquisition, processing, analysis, and interpretation of Helicopter Multi-sensor Towed Array Detection System magnetometry data for unexploded ordnance related sites at the former Kirtland Precision Bombing Range. The work was performed by Sky Research, Inc. of Oregon, with Dr. John Foley serving as Principal Investigator, and Mr. David Wright, formerly of AETC and now with Sky Research, serving as co-Principal Investigator.

Funding for this project was provided by the Environmental Security Technology Certification Program Office. This project offered the opportunity to examine advanced airborne methods as part of the Department of Defense's efforts to evaluate wide area assessment technologies for efficient the characterization and investigation of large Department of Defense sites.

We wish to express our sincere appreciation to Dr. Jeffrey Marqusee, Dr. Anne Andrews, and Ms. Katherine Kaye of the ESTCP Program Office for providing support and funding for this project.

## **1. INTRODUCTION**

### **1.1. Background**

Unexploded ordnance (UXO) contamination is a high-priority problem for the Department of Defense (DoD). Recent DoD estimates of UXO contamination across approximately 1,400 DoD sites indicate that 10 million acres are suspected of containing UXO. Because many sites are very large (greater than 10,000 acres), the investigation and remediation could cost billions of dollars. However, for many of these sites only a small percentage of the total area may be contaminated with UXO. Consequently, determining applicable technologies to define the contaminated areas requiring further investigation and munitions response actions could provide significant cost savings. Therefore, the Defense Science Board (DSB) has recommended further investigation and use of Wide Area Assessment (WAA) technologies to evaluate their utility in determining the actual extent of UXO contamination on DoD sites.

In response to the DSB Task Force report and recent Congressional interest, the Environmental Security Technology Certification Program (ESTCP) designed a Wide Area Assessment Pilot Program (WAA-PP) that consists of demonstrations of WAA technologies at multiple sites. The purpose of the demonstrations is to validate a comprehensive approach to WAA through the application of a number of recently developed and validated technologies, including high altitude airborne sensors (orthophotography and Light Detection and Ranging [LiDAR]), helicopter-borne magnetometry arrays, and ground surveys.

This report documents the demonstration of the Helicopter Multi-sensor Towed Array Detection System (MTADS) Magnetometry (HeliMag) technology for the entire WAA demonstration site at the former Kirtland Precision Bombing Range (KPBR) and conducted as part of ESTCP project MM-0535.

HeliMag provides efficient low-altitude digital geophysical mapping (DGM) capabilities for metal detection and feature discrimination at a resolution approaching that of ground survey methods, limited primarily by terrain, vegetation, and structural inhibitions to safe low-altitude flight. The magnetometer data can be analyzed to extract either distributions of magnetic anomalies (which can be further used to locate and bound targets, aim points, and open burn/open detonation (OB/OD) sites), or individual anomaly parameters such as location, depth, and size estimate. The individual parameters can be used in conjunction with target remediation to validate the results of the magnetometer survey.

### **1.2. Objectives of the Demonstration**

The purpose of this demonstration was to survey the WAA demonstration site at the former KPBR in areas amenable to low-altitude helicopter surveys. Specific objectives of this demonstration included:

- Identify areas of concentrated munitions, including the known and suspected target areas;

- Bound the target areas;
- Estimate density and distribution of munitions types and sizes;
- Characterize site conditions to support future investigation, prioritization, remediation, and cost estimation tasks.

A determination of success for this demonstration was based on the performance of the system, as described in Section 4.

### **1.3. Regulatory Drivers**

This site and the associated target areas are classified by the United States Government as a Formerly Used Defense Site (FUDS) under the Defense Environmental Restoration Program (DERP). Currently, the WAA study area is undeveloped. Portions are planned for commercial or industrial development within the next decade, and airport expansion into these lands is possible.

### **1.4. Stakeholder/End-User Issues**

ESTCP is managing the stakeholder issues as part of the WAA-PP. ESTCP uses a process that ensures that the information generated by the high airborne, helicopter, ground, and validation surveys is useful to a broad stakeholder community (e.g., technical project managers and Federal, State, and local governments, as well as other stakeholders).

## 2. TECHNOLOGY DESCRIPTION

### 2.1. Technology Development and Application

The Naval Research Laboratory (NRL) developed the MTADS technology. Use of this technology was transferred to Sky Research for commercialization via a Cooperative Research and Development Agreement (CRADA). Prior to the transfer, this technology was fully evaluated for the DoD by ESTCP (Nelson et al. 2005; Tuley and Dieguez 2005).

The HeliMag system includes a helicopter-borne array of magnetometers and software designed specifically to process data collected with this system and perform physics-based analyses on identified targets (Table 1). These technologies are described in greater detail in the following subsections.

**Table 1. Sky Research HeliMag Technology Components**

<b>Technology Component</b>	<b>Specifications</b>
Geophysical Sensors	7 Geometrics 822 cesium vapor magnetometers, 0.001 nanotesla (nT) resolution
GPS Equipment	2 Trimble MS750 GPS receivers, 2-3 centimeter (cm) horizontal precision
Altimeters	1 Optech laser altimeter and 4 acoustic altimeters, 1 cm resolution
Inertial Measurement Unit	Crossbow AH400, 0.1 degree resolution
Data Acquisition Computer	NRL Data Acquisition Computer
Aircraft	Bell Long Ranger helicopter

#### 2.1.1. Helicopter Platform

Sky Research used a Bell Helicopter Model 206 helicopter (Figure 1) for data collection at the former KPBR site. The helicopter platform was used to deploy the geophysical sensors, global positioning system (GPS) equipment, altimeters, inertial measurement unit (IMU), and data acquisition computer (DAQ) technologies listed in Table 1. The helicopter is typically deployed at survey altitudes of 1-3 meters (m) above ground level (AGL).

An onboard navigation guidance display (Figure 2) provided pilot guidance, with survey parameters established in a navigation computer that shared the real-time kinematic GPS (RTK GPS) positioning data stream with the data acquisition computer. The survey course was plotted for the pilot in real time on the display. The sensor operator monitored presentations showing the data quality for the altimeter and GPS and the GPS navigation fix quality. This allowed the operator to respond to both visual cues on the ground and to the survey guidance display. Following the survey, the operator had the ability to determine the need for surveys of any missed areas before leaving the site.



**Figure 1.** Helicopter MTADS technology as deployed on Bell Long Ranger helicopter at former KPBR.

### 2.1.2. Sensors and Boom

The MTADS magnetic sensors were Geometrics 822A Cesium (Cs) vapor full-field magnetometers (a variant of the Geometrics 822). The array of seven sensors was interfaced to NRL's DAQ and the sensors were evenly spaced at 1.5 m intervals on a 9 m Kevlar boom mounted on the helicopter. The boom used for this data collection was the NRL boom used in previous ESTCP demonstrations of the technology.

**Figure 2.** The track guidance system provides flight traverse information to the pilot.



### **2.1.3. Positioning Technologies**

Two Trimble MS750 RTK GPS receivers were used to provide positions and platform attitude at 20 hertz (Hz), with four acoustic altimeters for recording the altitude of the platform. An IMU was used to correct for platform pitch. The data acquisition system was aligned with the GPS Universal Time Coordinated (UTC) time. The GPS time stamp was used as the basis for merging position data with sensor information.

RTK GPS was also used to generate positions for ground surveying. Sky Research utilized an in-house professional land surveyor to ensure that geospatial data generated by the project maintained accurate ties to the local coordinate system.

### **2.1.4. Data Acquisition System**

Magnetometer, altimeter, and navigational instrumentation were streamed into a rack-mounted computer housed in the back seat of the helicopter (Figure 2). This computer ran a customized version of Geometrics MagLogNT data-collection software. The equipment rack also contained the GPS receivers and Geometrics G-822AS super counters, which controlled the sampling rates for the seven individual sensors. The magnetometer data are typically logged at 100 Hz, which provides a nominal down-the-track sample interval of 0.15 m at a typical survey speed of 15 m/second (m/s).

### **2.1.5. Data Processing**

Data were downloaded via computer disks and uploaded via the Internet after each survey mission. Data processing was performed using custom application software running under the Oasis Montaj (Geosoft Ltd., Toronto, Canada) geophysical data processing environment. An overview of this process is outlined in the flow diagram provided in Figure 3. The processing conducted as part of this demonstration is described in greater detail in Section 3.6.5.

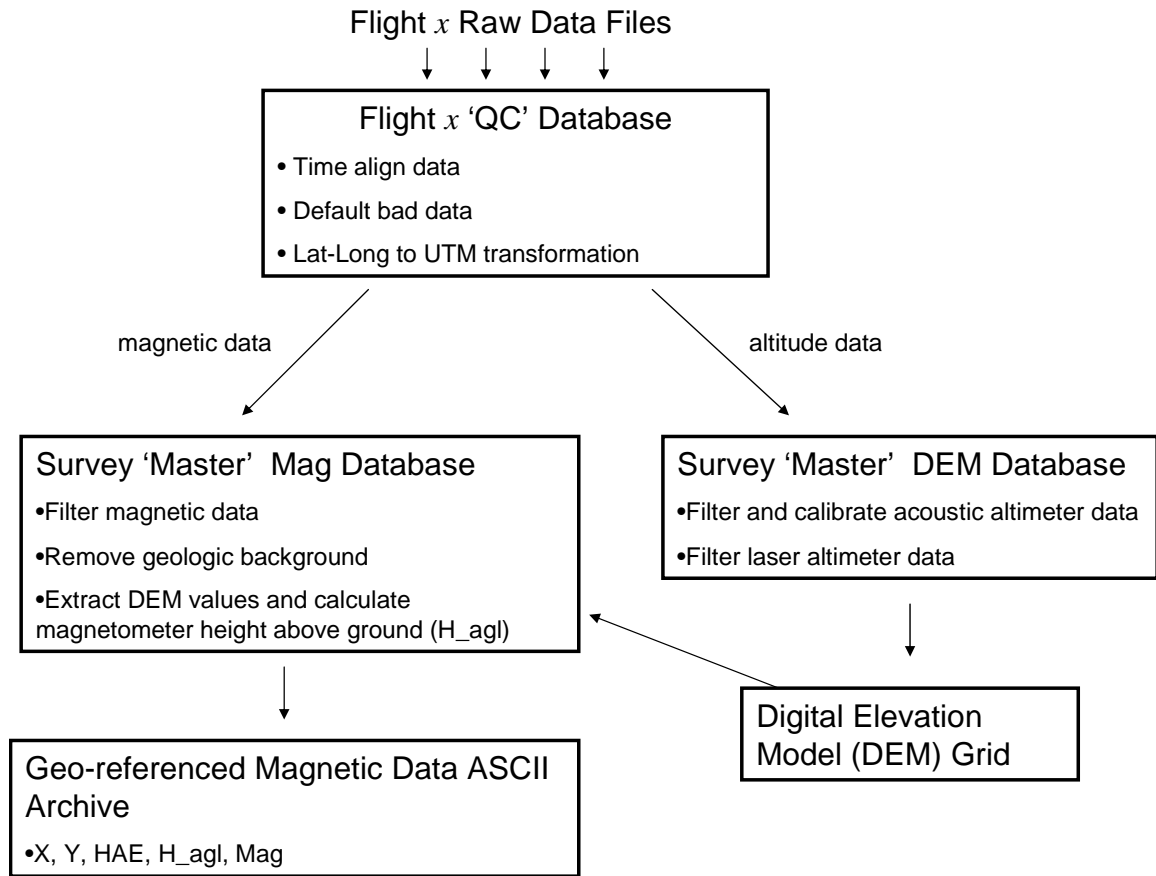


**Figure 3.** Helicopter MTADS processing flow chart.

### 2.1.6. Data Analysis

Once magnetic anomaly maps were created, anomalies were selected using an automated target selection methodology in Oasis Montaj. Automatic target selection for large-scale surveys such as this one has the advantage of being objective and repeatable as well as much faster than manual selection. However, automatic target pickers are not yet sophisticated enough to reliably detect closely spaced targets or targets that are at or below the same amplitude as local geologic signal. Therefore, to avoid selecting an excessive number of false targets, automatic target selection routines were only used to select targets with response amplitudes significantly above the background geologic noise. Furthermore, the automatic routines do not perform well in areas of high target density.

For the purposes of WAA where the main goal is to delineate target density throughout the survey site, the limitations of automatic target selection are not as detrimental as they would be if we were concerned with detecting every possible UXO target. The challenge is to calibrate the automatic target selection routine so that the number of valid targets of interest selected is maximized, while minimizing the number of targets selected due to geologic noise (or other noise sources). To achieve this, manual target selection results were compared with those

obtained using an automated target selection routine over a representative subset of the survey site. The results of the comparison were used to fine-tune the parameters for automatic target selection.

## **2.2. Previous Testing of the Technology**

Previous testing of the helicopter magnetometry technology in general was supported by ESTCP (Nelson et al. 2005). The primary development objective was to provide an UXO site characterization capability for extended areas, while retaining substantial detection sensitivity for individual UXO. The system included data collection hardware in the form of a helicopter-borne array of magnetometers, and software designed to process data collected with this system and to perform physics-based analyses on identified targets.

## **2.3. Factors Affecting Cost and Performance**

For any airborne survey, the largest single factor affecting the survey cost is the cost of operating the survey aircraft and sensors at the site. These equipment costs are related to capital value, maintenance overhead, and direct operating costs. In addition, mobilization and demobilization costs can be substantial. These costs increase with distance; some cost savings can be achieved if flexibility of scheduling is possible to share costs across several projects running consecutively.

The primary factors affecting performance are limitations imposed by topography, vegetation, geology, and weather. Helicopter surveys should not be used in areas where topography and/or vegetation limit the ability to safely conduct low altitude flights. The efficacy of the system can be diminished in areas where the magnetic geologic signal is sufficient to mask signals from our targets of interest. Last, weather can delay helicopter surveys, decreasing the daily production rate average and increasing the survey costs through standby day charges.

## **2.4. Advantages and Limitations of the Technology**

As with all characterization technologies, site-specific advantages and disadvantages exist that strongly influence the level of success of their application.

Advantages of HeliMag technologies include:

- the ability to characterize very large areas; and
- lower per-area cost than ground-based DGM methods.

Limitations of HeliMag technologies include:

- as a WAA tool, not intended to detect individual munitions and explosives of concern (MEC); and
- constraints on use due to site physiography, such as terrain, soils, and vegetation.

### **3. DEMONSTRATION DESIGN**

#### **3.1. Performance Objectives**

Performance objectives are a critical component of the demonstration because they provide the basis for evaluating the performance and costs of the technology. For this demonstration, both primary and secondary performance objectives were established. Table 2 lists the performance objectives for the helicopter MTADS technology, along with criteria and metrics for evaluation.

#### **3.2. Test Site Selection**

The selection of the former KPBR demonstration site as one of several demonstration sites in the WAA Pilot Program was based on criteria selected by the ESTCP Program Office in coordination with the WAA Advisory Group of state and federal regulators.

#### **3.3. Test Site History/Characteristics**

The former KPBR is a 15,246 acre FUDS used as a World War II-era military training facility. The WAA demonstrations were conducted on the 5,000 acre demonstration site located on either side of Double Eagle Airport. The physiography and known munitions-use history of the study area are discussed in detail in the Conceptual Site Model (CSM) (Versar 2005). Physiographic and historic military use characteristics most relevant to the technology demonstration are described briefly below.

The study area was known to contain three precision bombing targets identified as N-2, N-3, and New Demolition Impact Area (NDIA), as well as a simulated oil refinery target (SORT). The CSM did not indicate any munitions-related activity in the southern portion of the study area. The specific location of the SORT was unknown, but was thought to be somewhere in the north-central to western edge of the study area. Therefore, the demonstration was designed to encompass the known and suspected target zones (Figure 4).

Three additional areas (Figure 5) were surveyed at the request of the ESTCP Program Office in February, 2007. These areas included a survey on the NW edge of the demonstration site, a north-south linear corridor in the central part of the demonstration site along a road construction project, and an area in the NE of the demonstration site surveyed at the request of the U.S. Army Corps of Engineers Albuquerque District.

**Topography.** The WAA study area is on a relatively flat terrace at about 6,000 feet elevation (mean sea level) atop the Rio Puerco Escarpment, which falls away to the west of the site. To the east of the study area, several volcanic cinder cones rise about 300 feet above the surrounding terrain. Gently rolling terrain on the study area generally varies by less than 50 feet in elevation,

**Table 2. Performance Objectives**

<b>Type of Performance Objective</b>	<b>Primary Performance Criteria</b>	<b>Expected Performance (Metric)</b>
Primary/Qualitative	Ease of use and efficiency of operations for each sensor system	Efficiency and ease of use meets design specifications
Primary/Quantitative	Geo-reference position accuracy	Within 0.25 m
Secondary/Quantitative	Survey coverage	>0.95 of planned survey area
Secondary/Quantitative	Operating parameters (altitude, speed, overlap, production level)	1-3 m AGL; 15-20 m/s (30-40 knots); 10%; 300 acres/day
Primary/Quantitative	Noise level (combined sensor/platform sources, post-filtering)	<1 nT
Secondary/Quantitative	Data density/point spacing	0.5 m along-track 1.5 m cross-track
Secondary/Quantitative	MEC parameter estimates	Size <0.02 m; Solid Angle < 10°

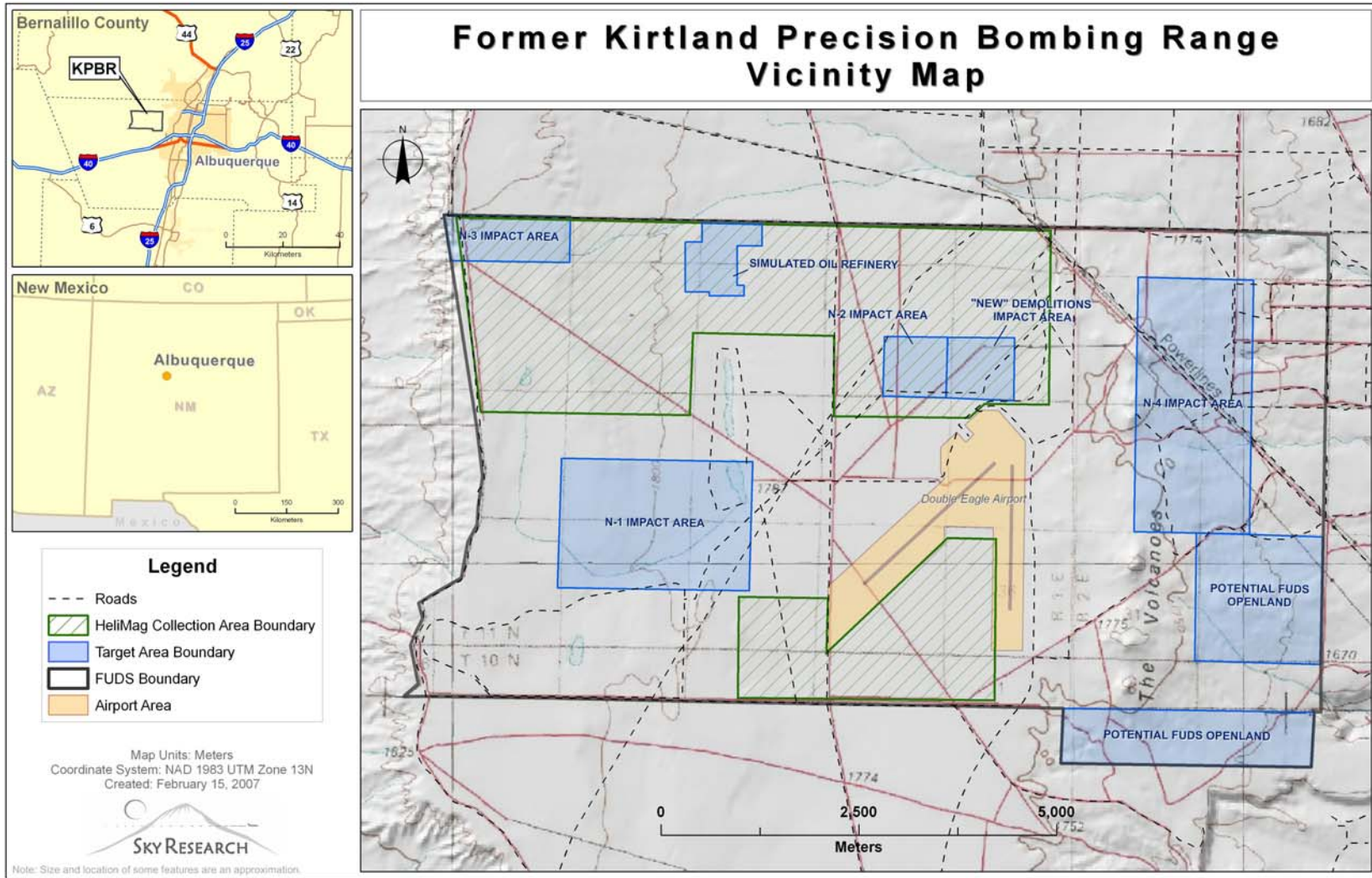


**Figure 4.** WAA demonstration area and helicopter survey boundaries for October 2005 HeliMag survey at the former KPBR.

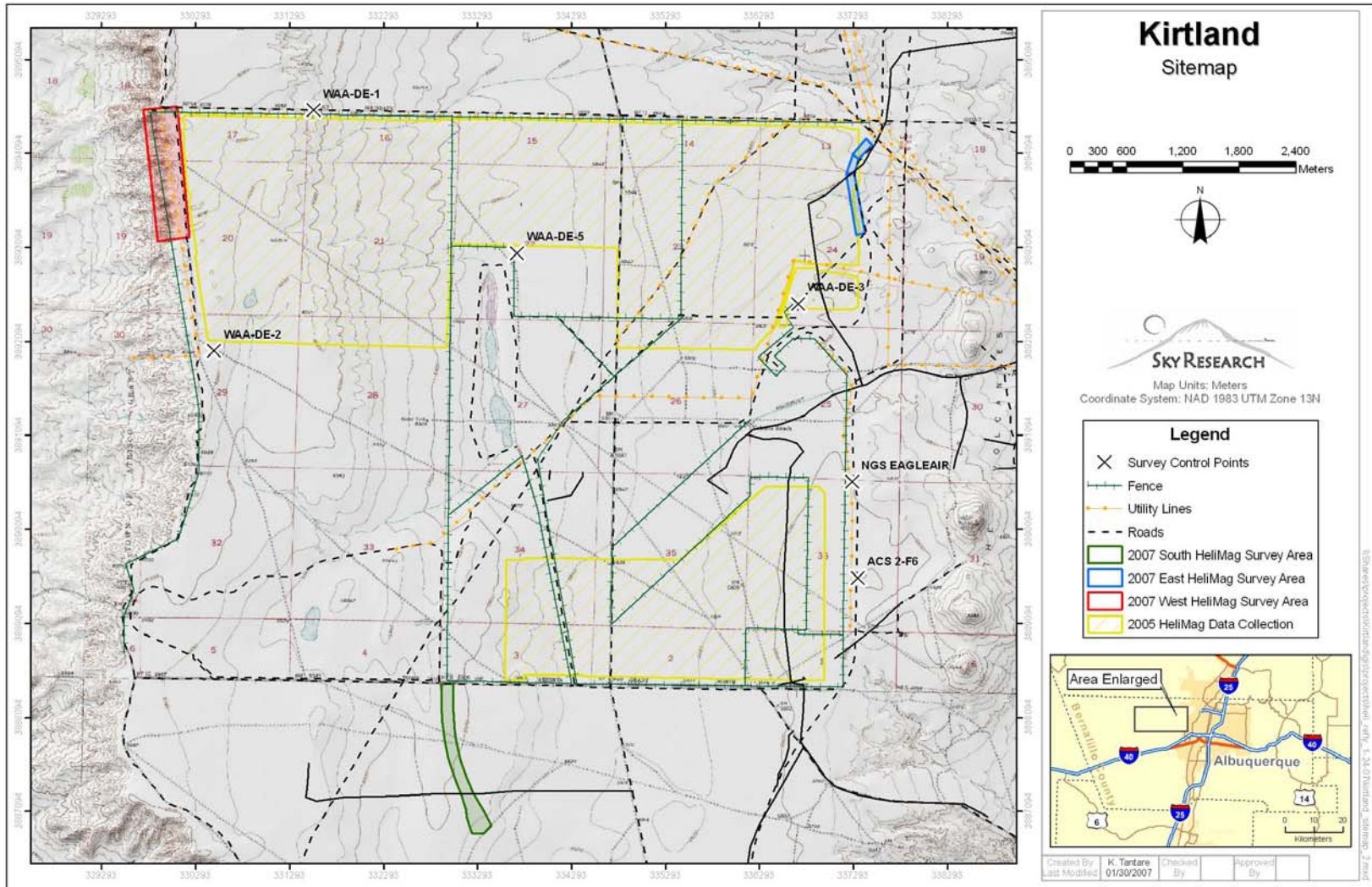


**Figure 5.** Three additional areas were surveyed in February 2007 shown with approximate boundaries shown in red, green and blue.

and is not incised by any significant drainage. Topographically, most of the site was amenable to low altitude helicopter surveys.

**Soils and Vegetation.** The soils within the WAA study area are deep, well-drained homogeneous sandy loams formed on loess parent material with low magnetic mineral content. The vegetation is short-grass prairie and cultivated fields with very few trees and shrubs; the vegetation did not pose a constraint to HeliMag operations.

**Climate and Hydrology.** The factors of summer thunderstorms and wind posed temporary scheduling constraints for HeliMag operations on the site during the period of planned operations. No surface hydrology factors existed on the site that inhibited WAA operations or provided a mechanism for MEC transport or burial.

**Land Use.** Land within the study area is primarily in City of Albuquerque ownership with minor portions owned by the State. Existing uses include portions of the site that are within the Double Eagle Airport boundary and within a recreational shooting range. A 1,200-acre sewage treatment soils amendment processing facility is located in the central area of the WAA study area and the airport is located in the eastern portion. Coordination of HeliMag activities with activities at the Double Eagle Airport was required. HeliMag activities near the shooting range required coordination with the City of Albuquerque.

**Cultural Features.** Utilities infrastructure crosses the study area, including several high-voltage transmission lines, two high-pressure natural gas transmission lines, water lines, an 8-inch gravity transmission sewage line, and a 6-inch natural gas pressure pipeline. Water wells, storage tanks, and transmission lines serving the airport fall partly within the WAA study area (Figure 5). Overhead electric transmission lines posed some constraints for HeliMag operations.

**Former Munitions Use.** Documented munitions present on the site surface within the study area include M38A2 and M85 100 pound (lb) practice bombs and spotting charges and 250 lb general purpose high explosive (HE) bombs. The primary aircraft in use at the site was the AT-11 bomber trainer which carried up to ten 100 lb practice bombs. The B-18 bomber was also reportedly used, which could carry a 4,000 lb payload of bombs. Aircraft flares were reportedly also dropped. Information in the Archive Search Report (ASR) indicates that a single 250 lb HE bomb was dropped “unofficially” by each trainee bombardier upon graduation from the training course, probably at the “New” target area east of the N-2 target area.

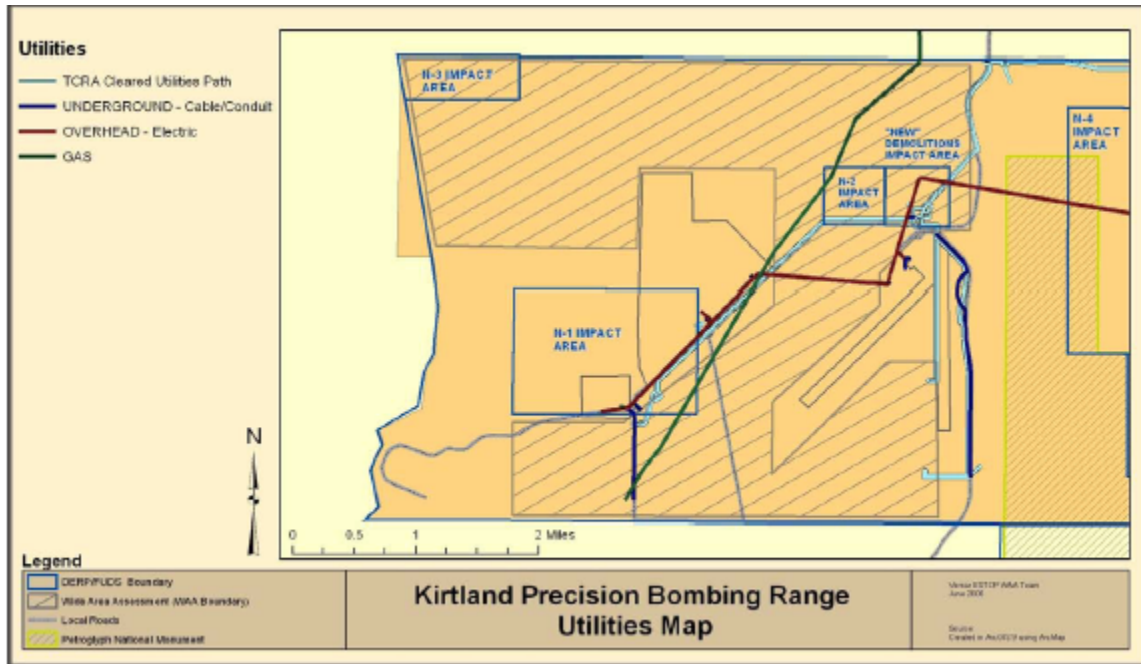


**Figure 6.** Utilities infrastructure present at the former KPBR.

The N-3 Target Area is a 320-acre half-section located near the northwest corner of the study area. It was known to contain the aiming circle of a precision bombing target. This target was cleared in 1952 and large pits within the area have been hypothesized as OB/OD areas. The presence of the target area was confirmed by concentrations of anomalies in the aiming circle as seen in HeliMag data; in addition, analysis of the data suggests secondary targets associated with N-3.

Additional known targets within the demonstration area include the N-2 Target Area and the “New” Demolitions Impact Area (NDIA) Target Area. The N-2 Target was documented as a 160-acre quarter-section containing a circular night bombing target including a power plant, underground cables, floodlight, and target circle. The NDIA target area is a target circle with high-explosives evidence. These targets were also seen in the HeliMag data.

The ASR indicates the presence of a SORT, but not its location or characteristics. Based on multiple data sets collected as part of the demonstration, the suspected location of the SORT is in the central part of the north area.

### 3.4. Present Operations

The WAA study area is currently undeveloped. However, portions of the study area are planned for commercial or industrial development within the next decade, and airport expansion into these lands is possible. Additional details about the Kirtland site can be found in the CSM.

### **3.5. Pre-Demonstration Testing and Analysis**

As discussed previously, the helicopter technology utilized for this demonstration is based on the NRL MTADS technology, transferred to Sky Research for commercialization via a CRADA. Prior to the transfer, this technology was fully evaluated by ESTCP (Nelson et al. 2005; Tuley and Dieguez 2005).

### **3.6. Testing and Evaluation Plan**

#### **3.6.1. Demonstration Set-Up and Start-Up**

Mobilization for this project required:

- 1) Mobilization of the equipment, pilot, and sensor operators.
- 2) Deployment of ground support personnel to establish ground fiducials, establish and operate GPS base stations, establish calibration line location, collect data on calibration location, and provide logistical support.

A base of field operations was established at the Double Eagle Airport, providing fuel and temporary hanger/storage space during operations at the site.

#### **Ground Control**

RTK GPS provided centimeter-accuracy real time positioning and was used with the HeliMag system. It was also used to generate positions for ground fiducials and for positioning ground calibration data and field verifications. The Sky Research in-house professional land surveyor ensured that geospatial data generated by the project maintain accurate ties to the local coordinate system.

#### **Sensor Calibration Targets**

The calibration line initially used at the site was the same calibration line constructed for the ground digital geophysical mapping used by another demonstrator. On the fourth day of the demonstration, Sky Research established a separate calibration line seeded with 8 targets seeded with a variety of calibration items (Table 3). The calibration lines were flown at the start and end of each of data collection survey and the resulting signatures compared to calculated responses to confirm the system operation. No targets were buried and no attempt was made to measure a probability of detection.

**Table 3. Calibration Items Seeded in the Calibration Lane**

<b>ID</b>	<b>X</b>	<b>Y</b>	<b>Azimuth</b>	<b>Description</b>
2001	336150.50	3892199.66	350°	Simulated 100 lb bomb
2002	336100.32	3892199.41	355°	155 mm projectile
2003	336049.92	3892199.93	10°	Metal cache box
2004	336000.56	3892199.55	355°	2.75" rocket
2005	335950.40	3892199.75	0°	Simulated 100 lb bomb
2006	335899.92	3892199.43	355°	155 mm projectile
2007	335850.62	3892199.49	5°	Metal cache box
2008	335800.55	3892199.69	0°	2.75" rocket

### **3.6.2. Period of Operation**

Pre-planning for the first survey was conducted in the summer of 2005, including submittal of the demonstration plan and final acceptance by the ESTCP Program Office. The ground surveys were conducted in September prior to mobilization of the ground crew and helicopter to the survey site. The helicopter was mobilized from Denver, Colorado, and the field crew mobilized from Ashland, Oregon. After arriving on site, the sensor boom was assembled and test flights conducted on October 2<sup>nd</sup>.

Data collection for the first survey occurred from October 3<sup>rd</sup> to 15<sup>th</sup>, 2005, and was completed in 11 flight days; two days during the data collection time period were downtime while waiting for access to the public gun club area. The airborne survey crew consisted of one pilot and one system operator; a second airborne survey crew was added on October 4-7 to increase daily productivity, with production reaching 674 acres on October 7<sup>th</sup> (Table 4).

Data collection for the second survey was concurrent with a deployment to survey portions of the Kirtland Air Force Base, and therefore no mobilization or demobilization was necessary for this project. The survey of the three additional areas was completed in one day of surveying, on February 25, 2007.

**Table 4. HeliMag Data Collection Acreage, 2005**

<b>Data Collection Day</b>	<b>Acres Surveyed</b>
October 3, 2005	387
October 4, 2005	546
October 5, 2005	643
October 6, 2005	655
October 7, 2005	674
October 8, 2005	451
October 9, 2005	186
October 10, 2005	457
October 11, 2005	560
October 14, 2005	158
October 15, 2005	285
<b>Acres Collected</b>	<b>5,002</b>
<b>Average Daily Productivity (acres/day)</b>	<b>454.7</b>

### **3.6.3. Area Characterized**

The October 2005 helicopter survey was conducted over 5,002 acres at the former KPBR. The second helicopter survey in February 2007 for the three additional areas was conducted over 353 acres. Figure 7 illustrates the combined HeliMag survey areas; the vertical scale represents the as-flown altitudes of the sensors (height above ground).

### **3.6.4. Operating Parameters for the Technology**

Sky Research deployed the airborne MTADS system on a Bell 206 Long Ranger helicopter platform, together with a pilot and system operator. A functionally identical system was deployed for the February 2007 surveys on a MD500E model helicopter. A ground support team operated the RTK GPS base stations. The helicopter was flown at a low altitude (1-3 m), with a forward velocity of 10 - 20 m/s.

As described previously, seven full-field Cs vapor magnetometers were deployed on the 9 m boom mounted transversely on the front of the helicopter skids. The DAQ logged data at 100 Hz. With the sensor spacing of 1.5 m and a speed over ground of 15 m/s, the resulting data density provides a minimum of 50 data points on a typical target to fit the dipole signature.

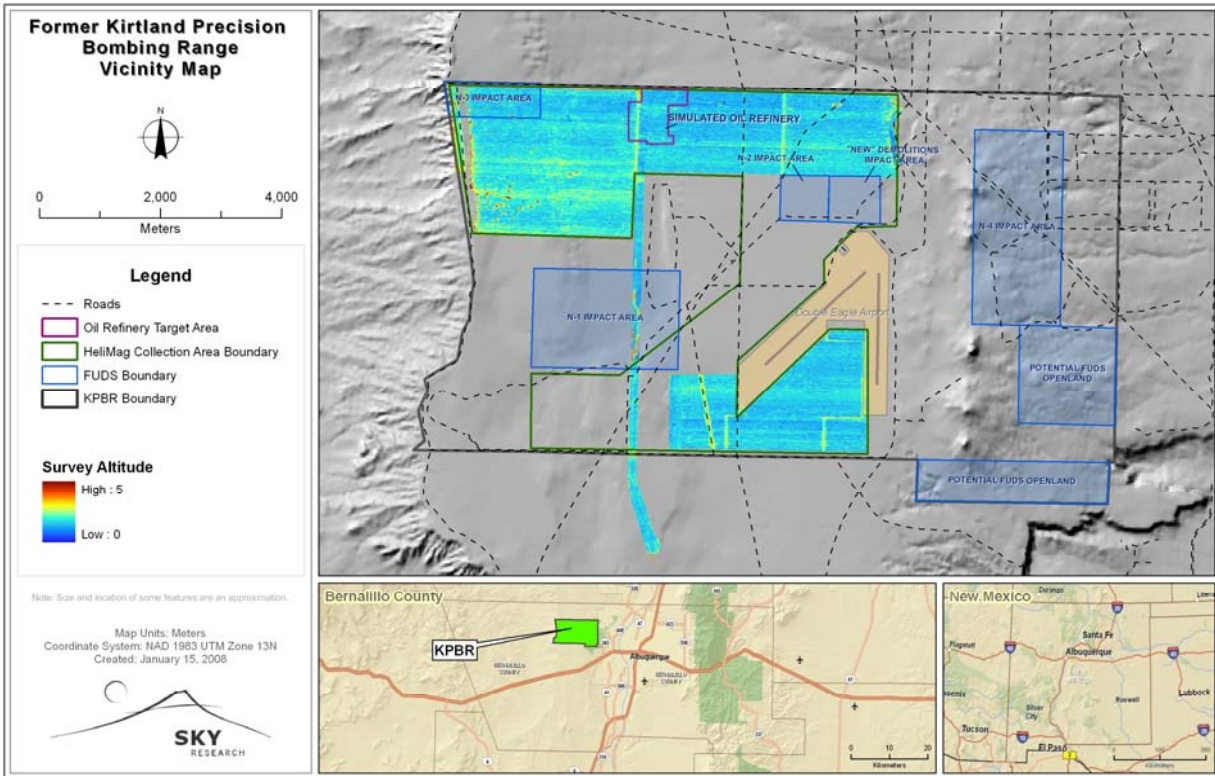


Figure 7. Map of as-flown HeliMag survey altitudes at former KPBR, 2005 and 2007.

### 3.6.5. Data Processing

Data processing for the 2005 survey was performed by AETC. During the first data processing stage, the raw data for a given survey flight were time-aligned and transcribed from the various raw data files into a 'flight' database. Routines were run to automatically reject or 'default' invalid data. Data were rejected based upon status flags present in the raw data records or, in the case of the magnetometer data, a simple 'in range' test was used. The GPS geographic position coordinates were transformed to WGS84 Universal Transverse Mercator (UTM) coordinates. At this point the data were visually inspected to ensure both integrity and quality. This pre-processing stage is instrumentation-specific and the steps required to transcribe these data into a time-aligned database were dictated by the structure of the data outputs from each device and the manner in which they were logged. All data outputs were received by the on-board DAQ. A DAQ time stamp was appended to each sample data string and the sample was then stored in a separate data file for each device. Table 5 provides a list of the raw data input files generated during the demonstration.

**Table 5. Helicopter MTADS Raw Data Input Files**

Device	Sample Rate (Hz)	Data Type	Filename extension	Remarks
Geometrics custom DAQ computer system trigger	100	TTL pulse	TriggerDevice.trig	Generated and logged by the DAQ – initiates the magnetometer sampling
Geometrics Model 822A Cs Magnetometers	100	RS232-ASCII	822A.Mag_a / 822A_Mag_b	7 magnetometers are controlled by 2 consoles – Mag_A sensors 1-4, Mag_B sensors 5-7
Trimble Model MS750 GPS position/attitude data	20/10	RS232-ASCII	GPS.nmea	Position data are in Trimble GGK message format, azimuth and roll are in Trimble AVR message format
Trimble Model MS750 GPS PPS (pulse per second)	1	TTL pulse	PpsDevice.pps	Used to accurately align integer GPS time with DAQ time
Trimble Model MS750 GPS time tag	1	RS232-ASCII	SerialDevice.utc	Used to resolve the integer ambiguity of the GPS PPS signal
Optech Model 60 Laser Altimeter	10	RS232-ASCII	SerialDevice.laser	Measures helicopter height AGL
Crossbow Tilt meter	10	RS232-Binary	SerialBinDevice.tilt	Used primarily for aircraft pitch measurement
Fluxgate magnetometer	10	RS232-ASCII	SerialDevice.fluxgate	Provides redundant aircraft attitude measurement
Acoustic altimeters	10	Analog voltage	AnalogDevice.analog	Measures sensor array height above ground level at two points

An important consideration for integration of the positioning system with geophysical sensors is that of time alignment. For dynamic applications, the time of applicability (TOA) of the geophysical sensor data must be aligned with the TOA of the measured positioning data to within one millisecond. Any measurement will have some latency before the data are collected and stored, which may be static or variable in nature. In addition to this latency, conventional time stamping of RS232 data is not precise and can inject hundreds of milliseconds of additional delays. Thus, simply time stamping the positioning data as it is transmitted to the DAQ does not ensure that the TOA of the positions can be precisely aligned with that of the geophysical data. When the Geometrics magnetometer consoles are triggered externally, the time lag between this external trigger and the TOA of the magnetometer samples is constant. Thus, using a trigger pulse generated by the DAQ allows determination of the TOA of the magnetometer data relative to the DAQ system time.

GPS systems commonly have an internal latency that is variable (i.e., the time between the applicability of a given measurement and the transmission of the derived position will vary) in

addition to the serial port variability. To allow users to know precisely when a measurement applies, the data message is time stamped (i.e., the position solution is given in 4 dimensions; time, x, y, and z) to a very high degree of precision. In addition, GPS receivers also output a pulse per second (PPS) trigger at every precise integer second to provide a means to synchronize the DAQ time with GPS time. The integer ambiguity of the PPS trigger is resolved by sending the data acquisition system a message (via RS232) that is simply used to assign the precise GPS integer time to the incoming PPS trigger. In this manner, GPS time may be precisely aligned with the DAQ system time.

The steps used to transcribe and time-align the raw data into a single flight database were as follows:

- 1) For each DAQ trigger event, the corresponding magnetometer data were read from the Mag\_A and Mag\_B files and stored as a database record. This record has seven magnetometer channels and a DAQ time channel.
- 2) The UTC time stamp was used to assign integer times to the GPS PPS data and these data were interpolated into a GPS time channel. This interpolation is based upon alignment of the DAQ time stamp assigned to each PPS with the existing DAQ time channel. This results in each sample of seven magnetometer readings having a corresponding DAQ time and GPS time record.
- 3) The GPS time channel and GPS time field in the raw data files were used to interpolate the GPS position and attitude data for each magnetometer sample. This results in the creation of the following channels in the database: Latitude, Longitude, Height above ellipsoid, GPS status, AVR yaw (angle of the sensor boom relative to true north), AVR roll (angle of the sensor boom relative to the horizontal plane), and AVR status. The geographic positions represent the positions of the master GPS antenna relative to the WGS84 ellipsoid. The GPS status and AVR status provide a quality of fit indication for the position and attitude data respectively.
- 4) The DAQ time channel and the DAQ time field in the raw data files were used to interpolate the ancillary data for each magnetometer record. The ancillary data channels include the following: laser, four acoustic altimeter channels (two for each acoustic altimeter station to provide redundancy), tilt meter pitch and roll, and fluxgate x, y, and z components.

After the data were transcribed, invalid data were defaulted to 'dummy' values. The magnetometer data were defaulted outside of a reasonable range and the GPS data were defaulted based upon the values of the two status flags. A four-point average filter was applied to the magnetometer data to remove the 25 Hz noise assumed to be vortex shedding. This noise is relatively small in amplitude (less than 0.5 nT) and, as a result, this filter has very little effect on the data.

Data processing with the use of Geosoft Oasis Montaj MTADS Processing Toolbox greatly speeds up the merging and data interpolating process due to the large database functionality and optimized merging algorithms. Typical production processing for 300-500 acres takes approximately eight hours of data processing to produce a raw data plot image.

During each day of the demonstration, the project data processor conducted an initial review of the geophysical data to ensure that the data were within a reasonable range, free from dropouts/spikes and timing errors, and otherwise apparently valid. Oasis Montaj software performs the review and provides the mean, maximum, minimum, and standard deviation for each data file. The summary was reviewed and the data visually inspected. If any problems existed, the project geophysicist assessed the problem(s) and made adjustments to the field operations as needed to ensure quality data collection. Additional processing steps after the raw data processing step include filtering, geologic trend removal, and smoothing if needed.

Data processing for the February 2007 survey was performed by Sky Research. The data processing methodology was functionally and materially the same and the data were handled in a manner consistent with the previous deployment.

### **3.6.6. Data Analysis**

The use of an automatic target picking methodology was investigated as part of this demonstration. Automatic target selection for large scale surveys such as this one has the advantage of being objective and repeatable as well as much faster than manual selection if a very large number of targets are to be selected. However, automatic target pickers are not yet sophisticated enough to reliably detect closely spaced targets or targets that are at or below the same amplitude as local geologic signal. Furthermore these automated routines are not able to differentiate among our targets of interest, local geologic anomalies, and non-UXO-like cultural sources (e.g. pipelines). In practice, the decision to pick manually, or use an auto-picker then add/reject targets manually is made based upon the number of targets to be picked and the extent of geologic/cultural clutter.

To investigate the use of automatic target picking for the former KPBR demonstration, a comparison of the results of an automated target picking procedure versus manual target picking results was conducted over a representative section of the demonstration site (Figure 8). The final total magnetic field data were used to create Geosoft style grid images with a grid cell size of 1 m.

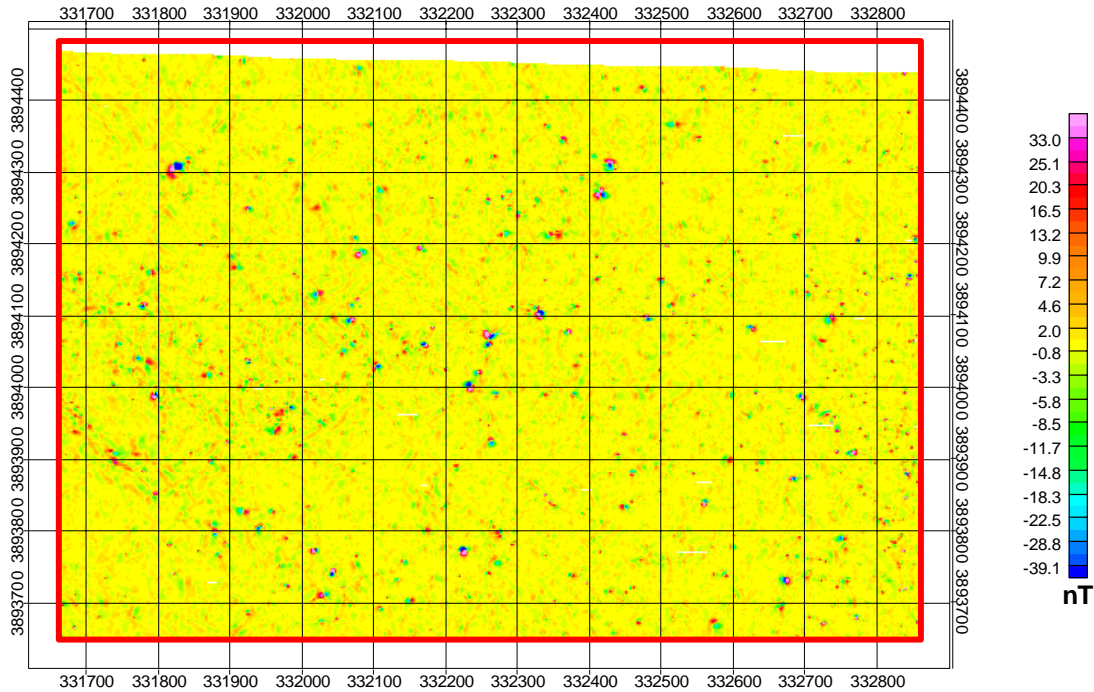


**Figure 8.** Total magnetic field grid image of the sample area used to calibrate the automatic target picking routine.

The Geosoft peak detection utility was used as the automated target detection routine. This GX uses the Blakely method to find peaks in a grid (Blakely and Simpson, 1986). This algorithm compares the value of each grid cell with values of eight (8) nearest grid cells in four directions (along the row, column, and both diagonals). If the value of the grid cell in question is higher than its neighbors, it is assumed to be a target. This routine is calibrated through the use of two parameters: the number of filter passes performed on the grid (to remove high spatial frequency noise a 3x3 Hanning filter may be applied a user-selectable number of times) and the minimum amplitude threshold below which no peaks are selected. Because of the dipolar nature of the total magnetic field response of our targets of interest, the total magnetic field grid was converted to a magnetic analytic signal grid. The analytic signal is the square root of the sum of the squares of the derivatives in the x, y, and z directions, and as such, results in a single peak anomaly over our targets of interest.

The Geosoft peak detection routine was run a number of times while varying the detection threshold (from 2 to 9 nT/m) and the number of passes of a 3x3 Hanning filter (from 0 to 3). The results from these tests were compared with the results obtained using manual target detection. Figure 9 shows the total number of targets selected using each method for each area and the sum of the two areas. The total number of targets is plotted as a function of the cut-off threshold used. A separate curve is used for each number of filter passes as well as for the manual method. The curve for the manually selected targets was determined by sampling the analytic signal grid, based upon the original manually selected coordinates, then binning the targets accordingly.

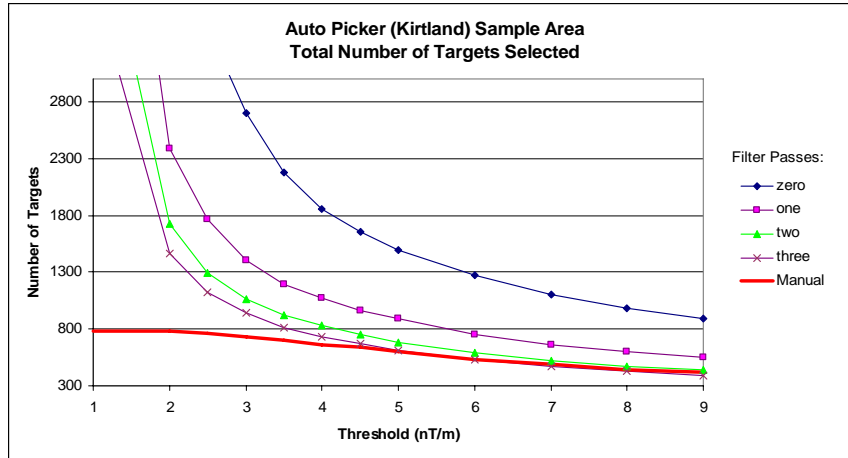


**Figure 9.** Total number of selected targets as a function of cut-off threshold amplitude.

At relatively high threshold values, the automatic target selection curves are similar to the manual selection curve (with the exception of the zero filter passes curve – clearly a minimum of one filter pass must be used). As the threshold is reduced below 5 nT/m (the point where the manual picker is marginally able to differentiate targets from geologic responses) the manual curve diverges radically from those of the automatic target selection routine. Using three filter passes does not appear to improve the auto-picker performance at lower thresholds (note that for each successive filter pass, the peak value for any given anomaly is reduced) and actually provides poorer performance at higher thresholds.

To provide an indication of the number of false target selections (relative to the number of true selections) as a function of target threshold, Figure 10 shows the total number of targets selected by the auto picker normalized by the number of manual picks as a function of cut-off threshold.

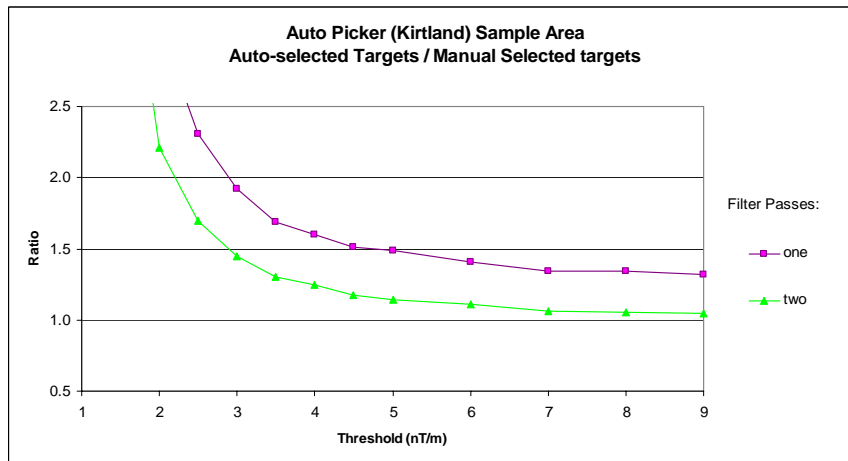


**Figure 10.** Number of targets automatically selected, normalized by the number of targets manually selected, as a function of cut-off threshold amplitude.

Based upon the data presented above and the calibration line results, it was decided that the appropriate parameters to use for the automatic target selection algorithm were two filter passes with a cut-off threshold of 4.5 nT/m. These parameters minimize the effect of geology on the target density map and maximize the number of valid targets selected.

### **3.6.7. Demobilization**

At the conclusion of the surveys, the helicopter, associated equipment, and field crews were demobilized from the site. Targets were investigated at a later date by a different contractor as part of the WAA validation surveys conducted on behalf of ESTCP.

## 4. PERFORMANCE ASSESSMENT

### 4.1. Data Calibration Results

#### 4.1.1. Data Calibration

The data collected over each target from the calibration line passes that are assumed to be valid (i.e., target positions are stable and data positioning quality is good) were analyzed with the MTADS dipole fit algorithm (using the UX Analyze environment). This analysis derives the parameters for a model dipole that best fits the observed data. These parameters include horizontal position, depth, size, and solid angle (i.e., the angle between the Earth's magnetic field vector and that of the dipole model). The derived parameters were examined for accuracy (determined as the average error where relevant) and repeatability (indicated by the standard deviation), as presented in Table 6.

**Table 6. Calibration Results for Calibration Lane Targets**

<b>Dipole Fit Parameter</b>	<b>Bias</b>	<b>Standard Deviation</b>
Easting	0.02 m	0.09 m
Northing	0.06 m	0.13 m
Depth	0.15 m	0.13 m
Size	n/a	7 mm
Solid Angle	n/a	6.0 °

Figure 11 shows the derived positions for each target relative to the ground truth supplied. The accuracy of these positions relative to the ground truth is well within the range expected for the MTADS system. The increased noise in the northing is assumed to be a result of the relative sample densities for each direction (the calibration lines were flown in an east-west direction and along-track sample density is 5 to 10 times higher than for across-track). This is consistent with our findings from the Pueblo calibration line data where the lines were flown in a north-south direction and the easting positions showed more variation.

#### 4.1.2. Calibration Item Response

In the dipole fit depth estimates (Figure 12) it appears that the depths are too deep by an average of 0.15 m. As surmised similarly for the Pueblo Precision Bombing Range demonstration of HeliMag technology, this bias in the calibration line results is most likely due to the grassy vegetative cover over the calibration area.

The dipole fit size estimate for any given munitions item will vary considerably depending upon the alignment of the object with the Earth's magnetic field. Therefore the size can only be used as a coarse estimate of the object size. For this reason, the accuracy of the size estimate of the calibration items is not of particular import when discussing the system performance, other than simply verifying that the estimate falls within the expected range for a given target (which they do, as shown in Figure 13). Because the calibration data consist of repeated flights over the same

stationary targets, the repeatability of the derived size estimates demonstrates consistency in system performance.

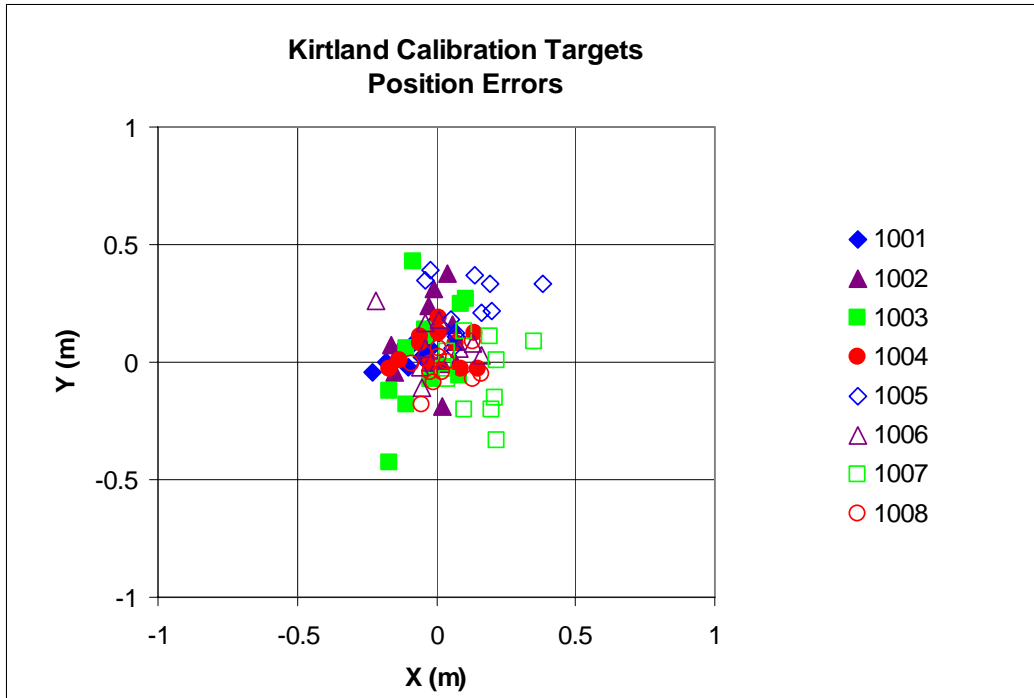


Figure 11. Derived positions for each target relative to the ground truth supplied.

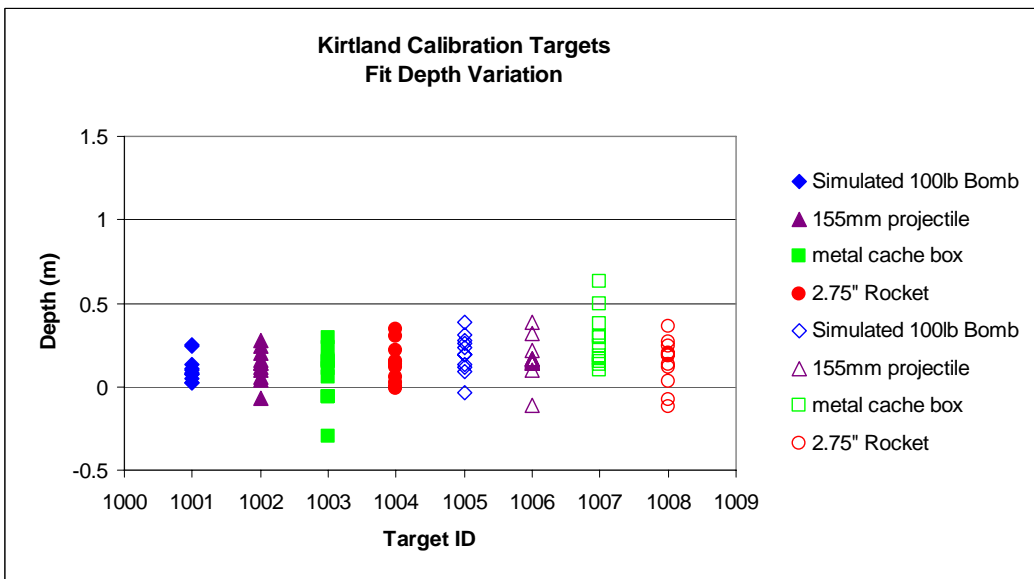
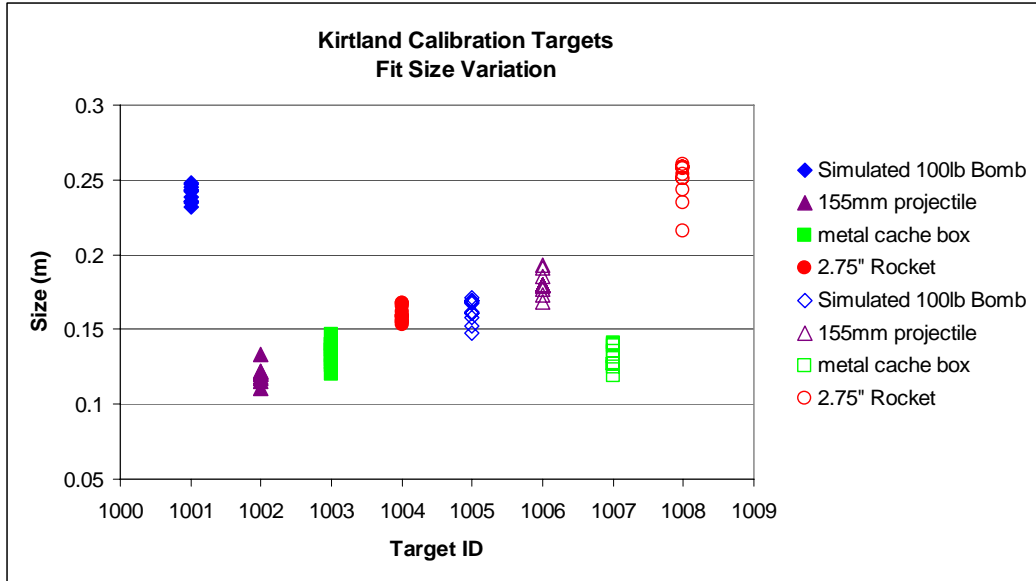
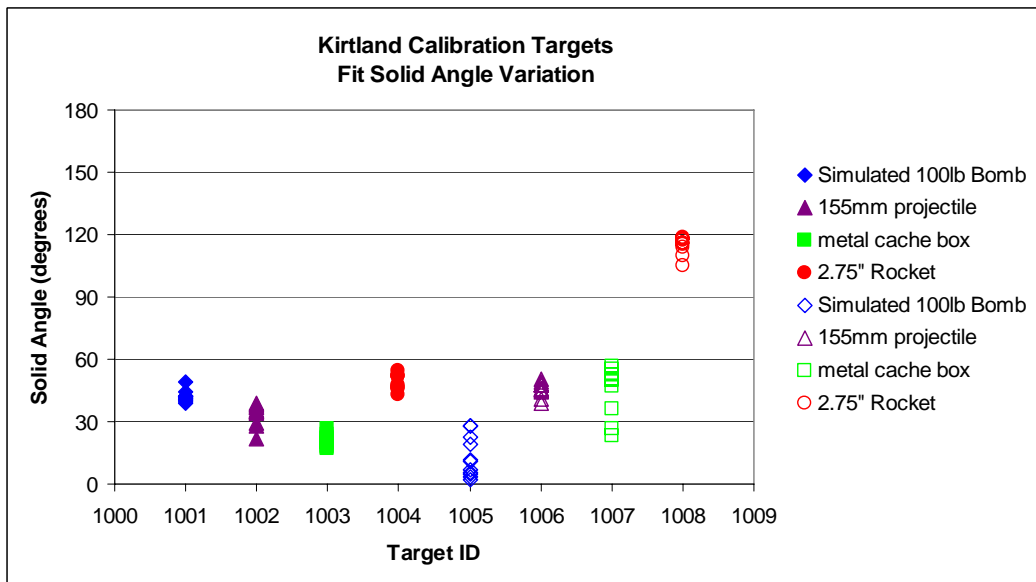


Figure 12. Dipole fit depth estimates for calibration line targets.



**Figure 13.** Dipole fit size estimates for calibration line targets.

In a manner similar to the size estimates discussed above, the dipole fit solid angle estimates depend heavily on the orientation of the target relative to the Earth's magnetic field. In the case of the calibration line test targets, the 'ground truth' is unknown and not important. However the stability of this prediction for repeated flights over the calibration line is indicative of the performance of the airborne system (Figure 14).



**Figure 14.** Dipole fit solid angle estimate for calibration line targets.

In addition to determining the repeatability of analyses performed on the calibration targets, the data collected over the targets can also be used to confirm the utility of the automatic target picking routine that is employed on the data sets to derive target density maps. The automatic target picker performs peak detection on a Geosoft style grid of the magnetic analytic signal that is in turn derived from a grid of the total magnetic field data. Prior to producing the analytic signal grid, the total magnetic field data were upward continued by 0.75 m to simulate burial of the targets by the same amount. The peak detection algorithm first applies a 3 x 3 Hanning filter to the analytic signal grid to remove very high spatial frequency features (local noise) so that multiple peaks are not detected in the vicinity of a true peak. The number of applications of this filter is optional. A second parameter used is the minimum threshold for peak detection. Testing of this peak detection routine has shown that the optimal number of filter passes is two and the nominal threshold value should be around 5 nT/m. Figure 15 shows the peak amplitudes for multiple passes over the calibration targets.

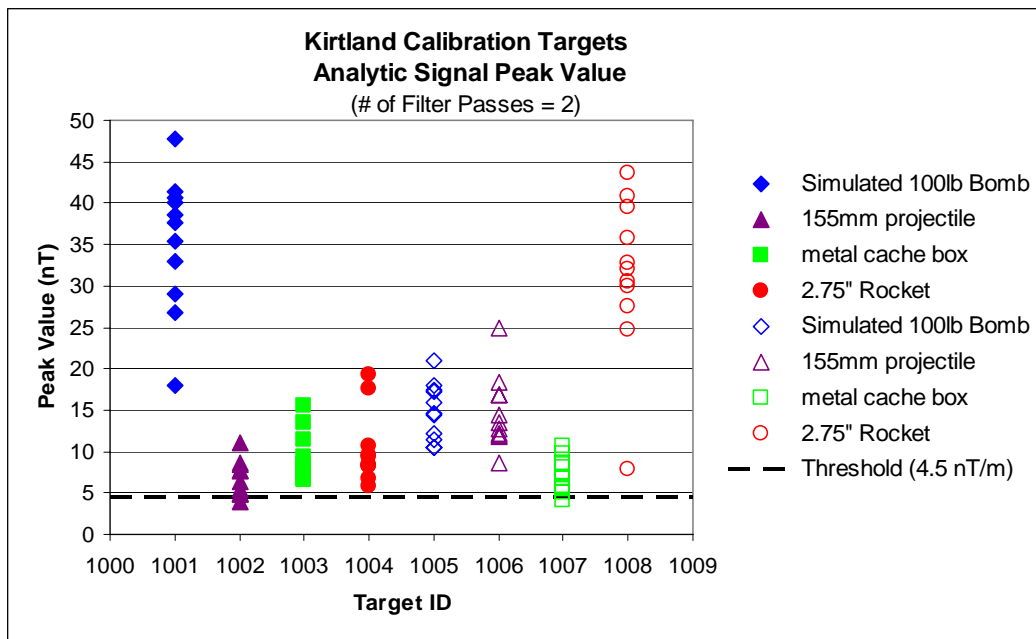


**Figure 15.** Peak analytic signal response for the calibration line targets after upward continuation of the magnetometer data to simulate 0.75 m burial of targets.

## 4.2. Overall Results

### 4.2.1. Anomaly Picking Results

For the purposes of WAA, the main goal is to delineate target density throughout the survey site. Target selection can be accomplished either manually or through automated routines; the geologic background signal largely determines what methods are best for a given site. Manual target selection is both subjective and labor intensive. The results obtained will vary considerably

depending upon the skill level of the analyst; even an experienced analyst will find it difficult to be consistent with respect to his/her ability to select targets that are masked by geologic signal or overlapping signal from other targets. In areas of “quiet” geologic background, automatic target pickers can be faster to use, scientifically repeatable and more objective than manual target picking.

Automatic target pickers are not yet sophisticated enough to reliably detect closely spaced targets or targets that are at or below the same amplitude as local geologic signal. Where a reasonably experienced analyst is able to successfully discriminate a large number of targets from localized geologic signals that are of the same amplitude or higher, the automatic target detection routines that are currently available are not able to differentiate between our targets of interest and local geologic anomalies. As a result, automatic target selection routines must only be used to select targets with response amplitudes significantly above the nominal geologic noise; otherwise, an inordinate number of false targets are selected. Furthermore, the automatic routines do not perform well in areas of high target density.

In practice, the decision to pick manually, or use an auto-picker then add/reject targets manually is made based upon the number of targets to be picked and the extent of geologic/anthropologic clutter that must be dealt with. Using the automated picking methodology described in Section 3.6.6, 23,648 anomalies were selected from the data from the 2005 survey to assess the distribution of metal objects across the study area. 5,300 anomalies were selected from the data from the 2007 survey to assess the distribution of metal objects across the three additional survey areas. Figure 16 illustrates the locations of these anomalies over all areas surveyed. A detailed description of each area of interest for both surveys is provided in Section 4.3.

#### **4.2.2. Metal Density Analysis**

To visualize the distribution of metal objects across the study area, a density raster was computed using a 100 m radius neighborhood kernel that assigned anomaly densities in anomalies per hectare to each cell in the raster. Simply described, at grid nodes of every two meters the number of targets that appear within a 100 m search radius were counted. This search radius provides the density in targets per 31,416 m<sup>2</sup>. These values were then ‘normalized’ by dividing by 3.1416 to provide density estimates in targets/hectare. The resulting data were gridded to provide anomaly density images. Figure 17 shows the anomaly density across all areas surveyed at the site.

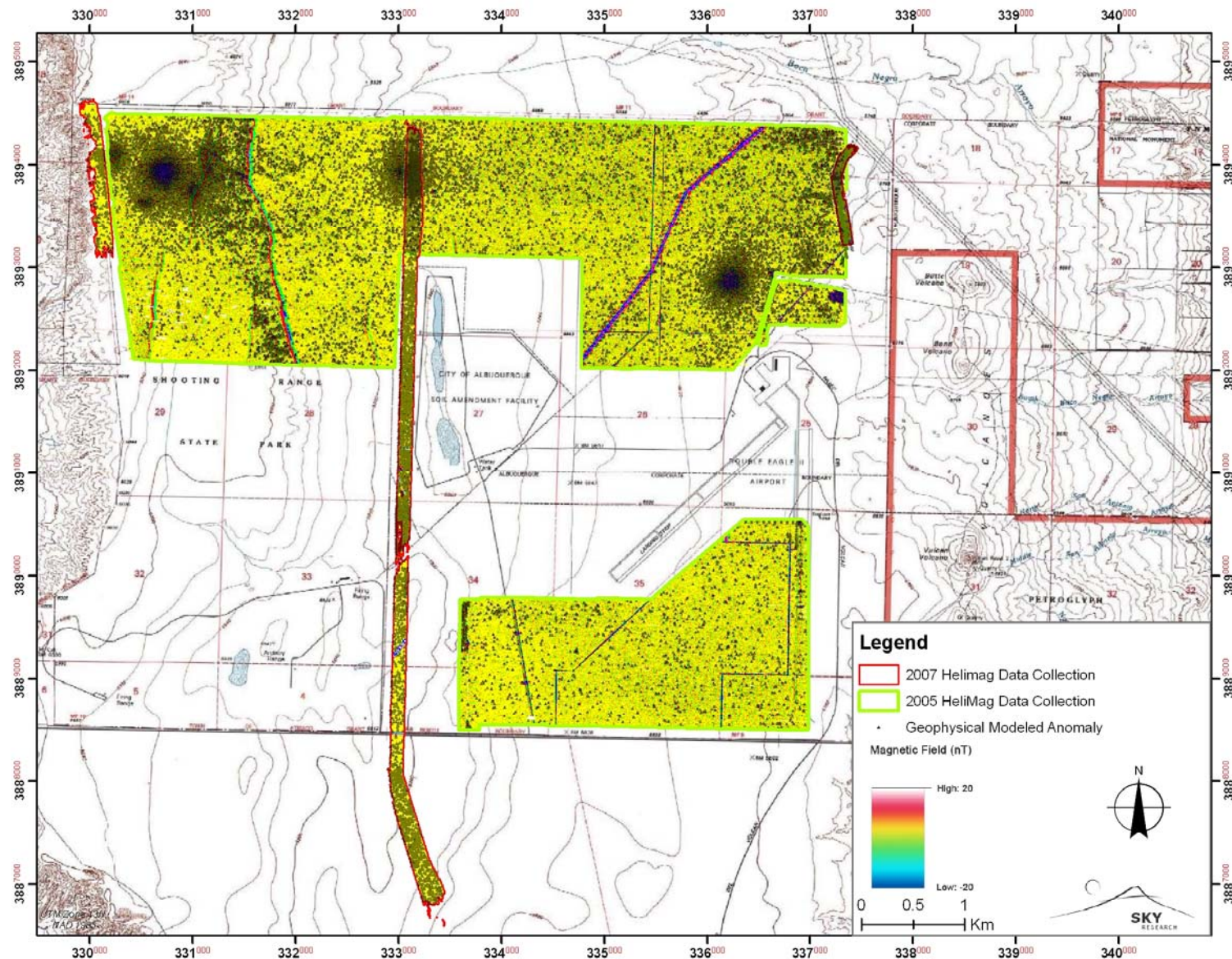


Figure 16. Geophysical anomalies shown overlain north and south study area on the total field geophysical data.

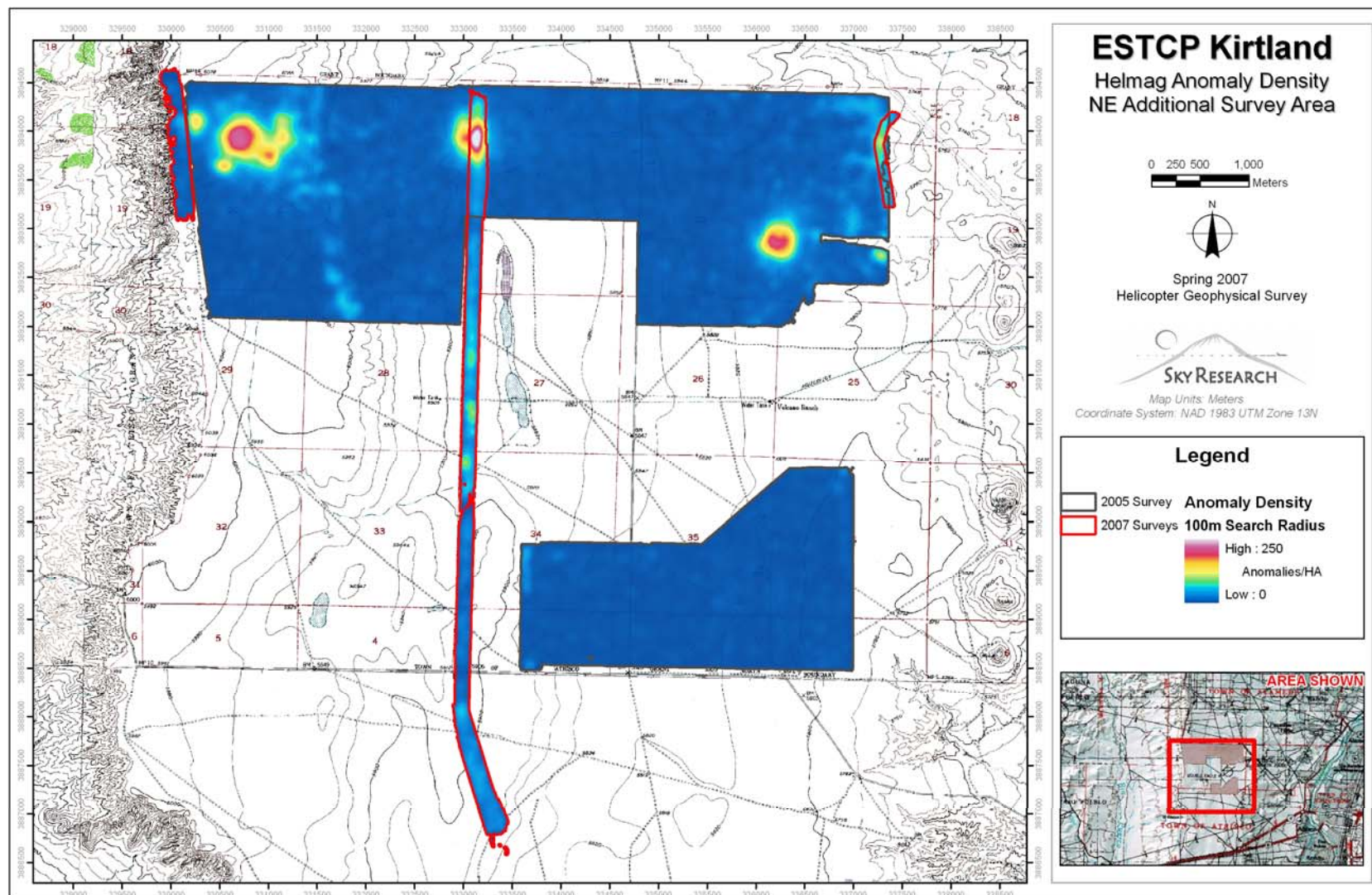


Figure 17. HeliMag anomaly density across all areas surveyed at the former KPBR.

### 4.2.3. Target Dipole-Fit Analyses

A subset of anomalies in each of the areas of interest were analyzed using the dipole fit analysis described in Section 4.1.1. These fit results were used to down-select candidate targets for intrusive investigation. Although a range of target sizes were picked, this subset of targets may not be entirely representative of a typical cross section of targets in these areas. We will however, attempt to relate the dipole fit results to the expected character of MEC at each site as presented in the original Conceptual Site Model (CSM) .

### 4.2.4. Intrusive Investigation Results

A number of targets were selected for intrusive investigation to supply ground truth. The dig program included anomalies detected by both the HeliMag system and the vehicular towed system (not a Sky Research endeavor). The dig results are tabulated in Table 7. The results from the HeliMag targets are also presented in chart form in Figure 18. From Figure 18 we can see that the dominant source of ferrous material in the areas chosen for intrusive investigation is MEC-related. In Table 6 we see significant differences between the HeliMag and Vehicular system results with respect to the percentage of non-UXO related scrap and percentage of no-finds. These discrepancies are assumed to be due to differences in the target sampling criteria used for selection of the subset of targets for each system.

**Table 7. Dig Results Comparison for HeliMag and Vehicular Towed System**

<b>Dig Result</b>	<b>HeliMag</b>	<b>Vehicular</b>	<b>Combined</b>
Intact UXO	5 (1%)	0 (0%)	5 (1%)
UXO related scrap	322 (81%)	244 (64%)	566 (73%)
Non-UXO related scrap	16 (4%)	48 (13%)	64 (8%)
No-finds	56 (14%)	87 (23%)	143 (18%)
<b>Totals</b>	<b>399</b>	<b>379</b>	<b>778</b>

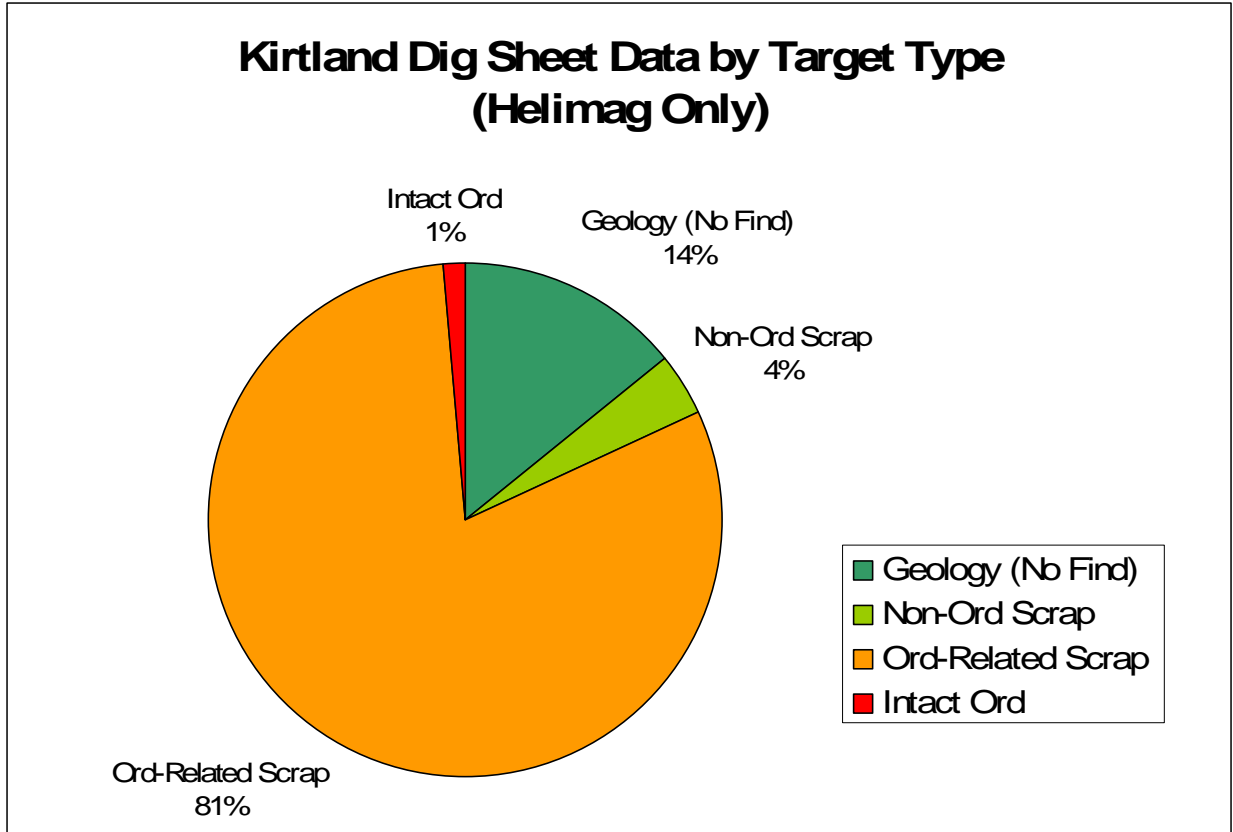


**Figure 18.** Intrusive investigation results for all selected anomalies. These results are an aggregate of the results from each area selected for intrusive investigation.

### 4.3. Results Discussion by Area

#### 4.3.1. Target N-2 Area

The helicopter magnetometry data clearly show high concentrations of anomalies throughout the N-2 target circle area. The number of anomalies detected within the CSM boundaries was 3,514. In Figure 19 we can see that the spatial extent of elevated ferrous material density is centered roughly on the target circle presented in the CSM. The original CSM, based upon visual reconnaissance, defined this extent to be elongated in nature and to have approximate dimensions of 1,500 feet (ft) (500 m) by 500 ft (150 m). From Figure 19 we see that the extent of elevated density is roughly circular in nature with an approximate diameter of 1,300 ft (400 m).

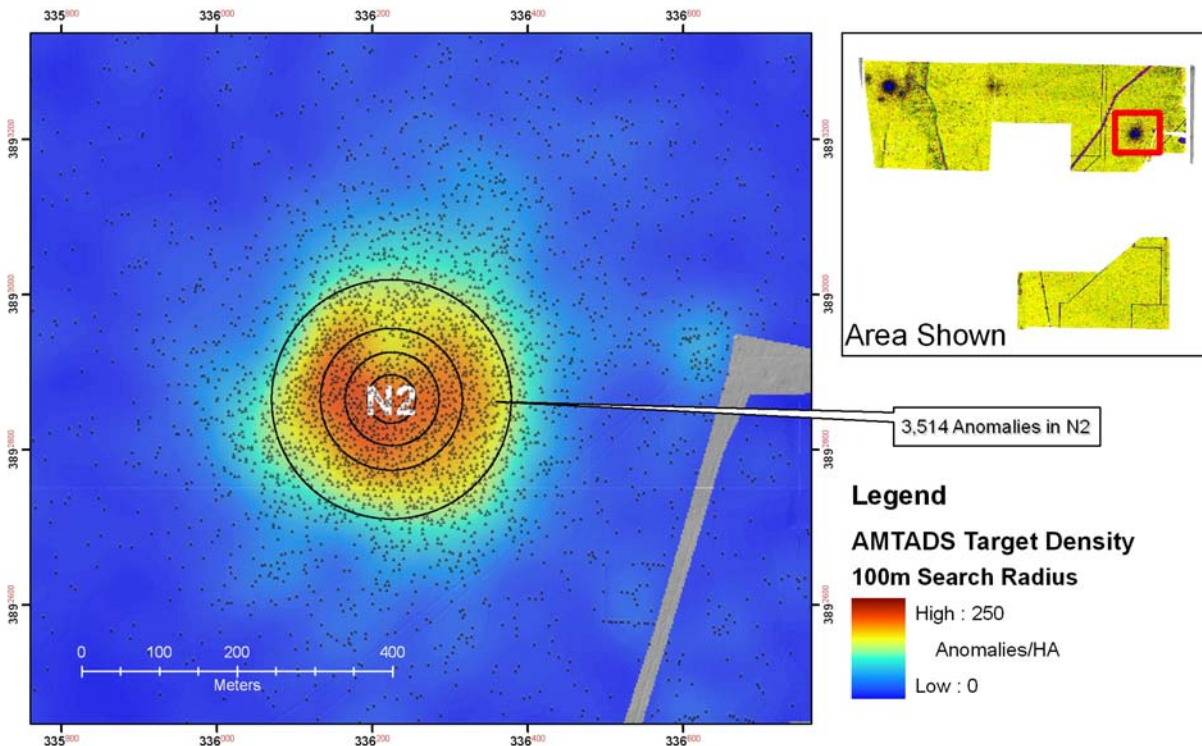


**Figure 19.** HeliMag target density and anomalies in the N-2 target area identified in the CSM.

#### 4.3.2. Target N-3 Area

HeliMag survey results showed that the extent of N-3 was not a single elongated impact area as originally identified in the CSM V0. The main impact area appears to be circular with a number of smaller ‘satellite’ areas of elevated concentrations. Based upon these results, an additional survey was conducted along the western boundary in 2007 to determine the full extent of the elevated density regions in this area (Figure 20). It is unclear whether the ‘satellite’ regions are due to separate bombing activities or whether they are a result of storage of MEC-related scrap associate with the original impact area.

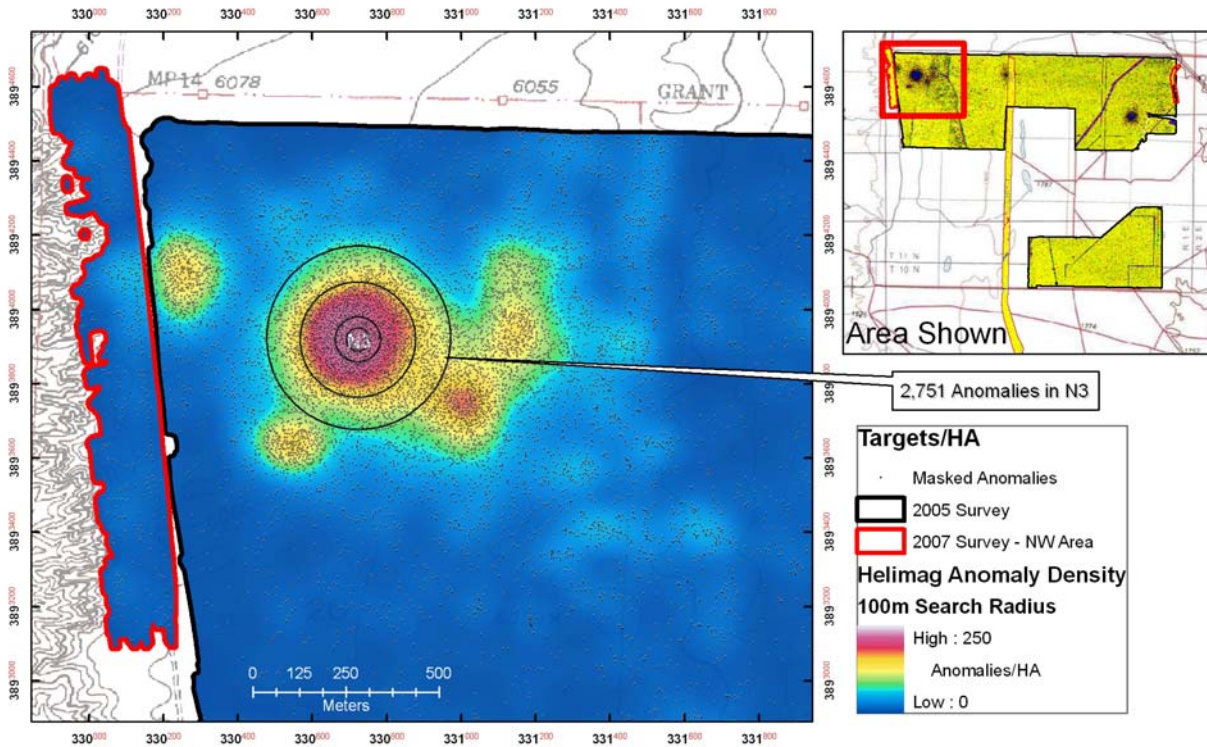


**Figure 20.** HeliMag target density and anomalies in the N-3 target area identified in the CSM.

The impact area does not appear to be elongated as target areas. Some of the smaller ‘satellite’ high anomaly density areas may be due to the storage of MEC as described in the CSM,

The intrusive results summarized in Figure 21 confirm the CSM with respect to the type of ordnance found at N-3. Out of a total of 273 targets investigated, 258 (95%) were found to be ordnance related scrap - all of which were identified as M38 parts or 100 lb bomb parts. Four (2%) inert 100 lb bombs were found, and the remaining 3% of the intrusive investigations resulted in no-finds of non-UXO related scrap.

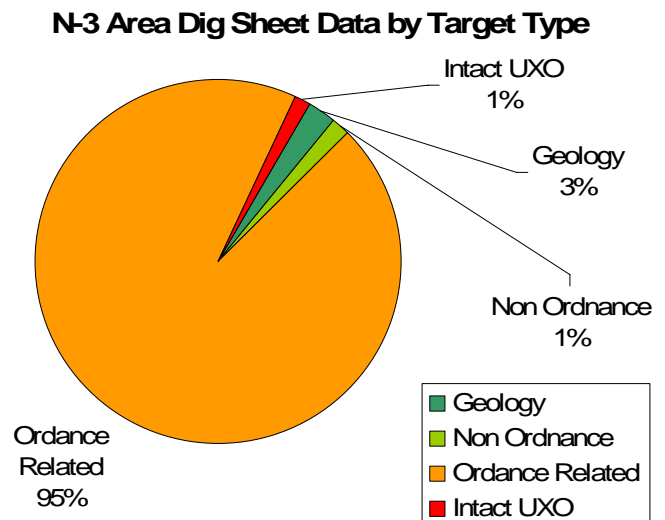


**Figure 21.** Intrusive investigation results for the N-3 area.

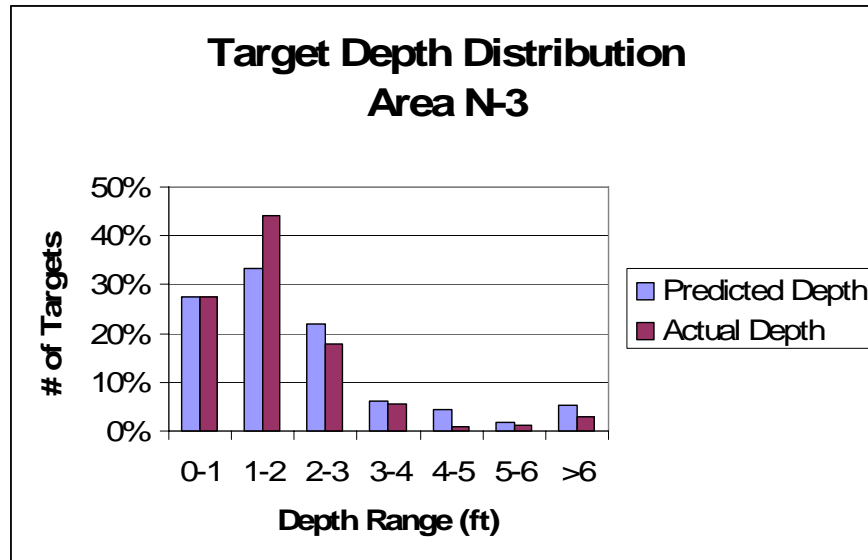


**Figure 22.** Depth distribution for targets investigated at the N-3 impact site.

In Figure 22 we show that the majority of targets (85%) do not exceed 3 ft (1 m) burial depth, and 95% of the targets are predicted to be within 5 ft of the surface. This is consistent with the assumptions made in the CSM. The slight shallow bias of the ‘actual depths’ compared to the predicted depths may be due to the fact that some distributions of multiple small shallow targets may model as a larger deep target.

#### 4.3.3. SORT Area

Within the CSM boundaries of the SORT area, 793 anomalies were detected; the metal density analysis shows a roughly circular area of high anomaly concentration centered just south of the midline of the western boundary (Figure 23). The area appears to be slightly distorted with a N-S bulge but this is probably due the fact that the data the 2007 fill-in data (flown parallel to a N-S fence line) were flown lower to the ground than the E-W lines flown in 2005.

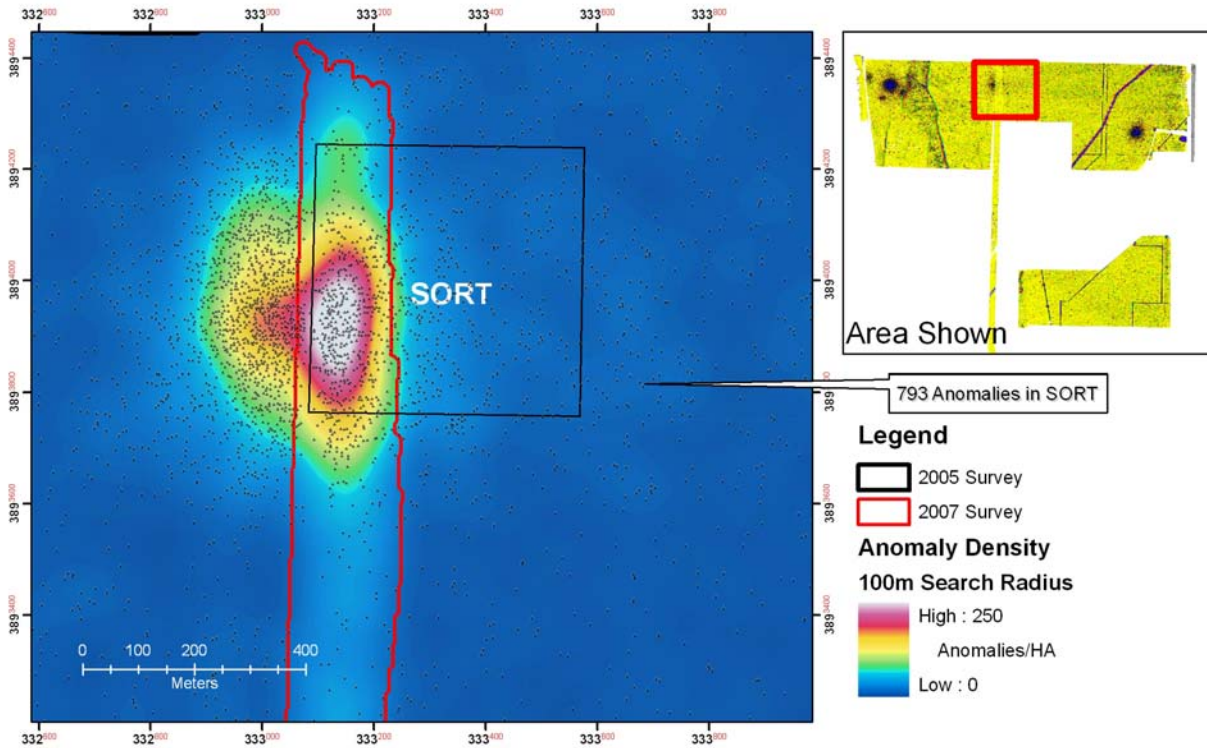


**Figure 23.** HeliMag target density and anomalies in the SORT area identified in the CSM.

There were a total of 56 anomalies investigated at the SORT area (summarized in Figure 24). Of these targets 1 (2%) was an intact inert M38 practice bomb, 2 (4%) were non-ordnance related scrap, 7 (13%) were ‘no-finds’ and 46 (82%) were ordnance related scrap – all of which were identified as M38 scrap. These findings confirm the CSM assumption with respect to ordnance usage at this site.

In Figure 25 we show that the majority of targets (72%) do not exceed 3 ft (1 m) burial depth, and 95% of the targets are predicted to be within 5 ft of the surface.

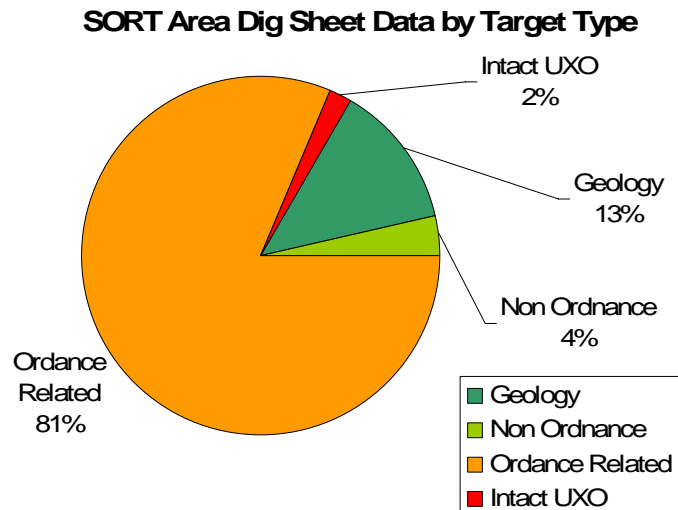


**Figure 24.** Intrusive results for the SORT area.

This is consistent with the assumptions made in the CSM. The slight shallow bias of the ‘actual depths’ compared to the predicted depths may be due to the fact that some distributions of multiple small shallow targets may model as a larger deep target. Also it bears mention that all of

the targets that were predicted to be deeper than 5 ft were found to be no-finds and assumed to be geologic in origin.

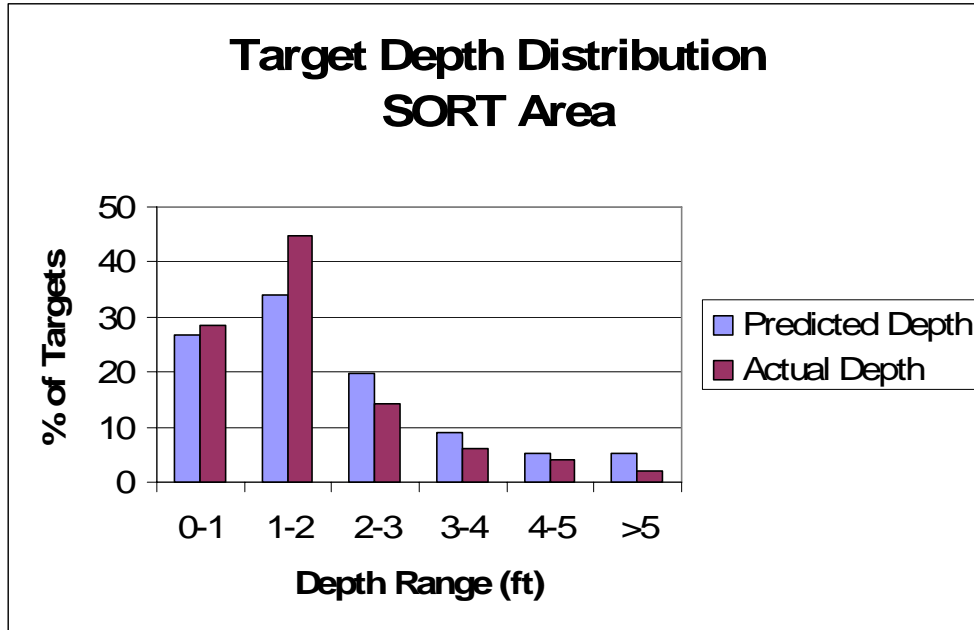
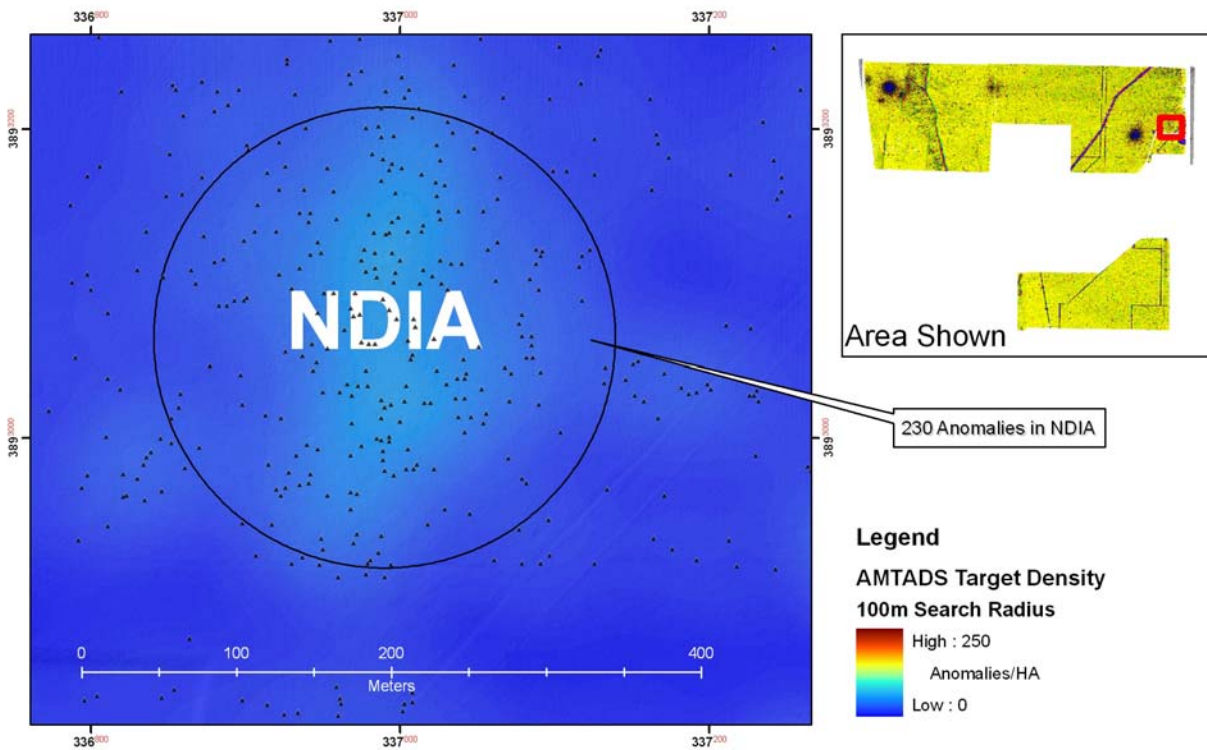


Figure 25. Depth distribution for targets investigated at the N-3 impact site.

#### 4.3.4. NDIA Area

Within the CSM boundaries of the NDIA area, 230 anomalies were detected. The NDIA area target density is considerably lower than the other impact areas. In Figure 26 we see a region of slightly elevated target densities (50 to 70 anomalies/Ha) elongated in a north-south orientation.



**Figure 26.** HeliMag target density and anomalies in the NDIA area identified in the CSM.

There were a total of 78 targets intrusively investigated at this area (summarized in Figure 27). Of these targets 13 (16%) were non-ordnance related scrap, 8 (10%) were ‘no-finds’ and 56 (71%) were ordnance related scrap – all of which were identified as M38 scrap. The significantly lower percentage of UXO-related finds relative to that found in the N-3 and SORT areas is in keeping with the lower over all anomaly density at this site (assuming that the ‘background’ anomaly densities are similar for each region). These results confirm the CSM prediction of lower contamination levels.

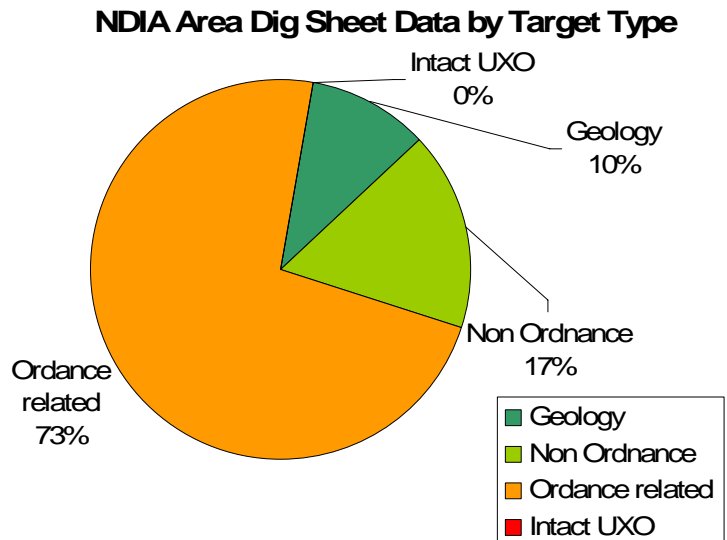


**Figure 27.** Intrusive results for the NDIA area.

In Figure 28 we show that the majority of targets (95%) do not exceed 3 ft (1 m) burial depth. This is consistent with the assumptions made in the CSM. The significant discrepancy between the predicted and observed depths may be explained by the relatively large number of non-UXO related items that typically have more complex shapes, thus are not as easily modeled. In addition, because only a small subset of targets were selected for investigation, analyst bias when picking targets may also contribute to this result.

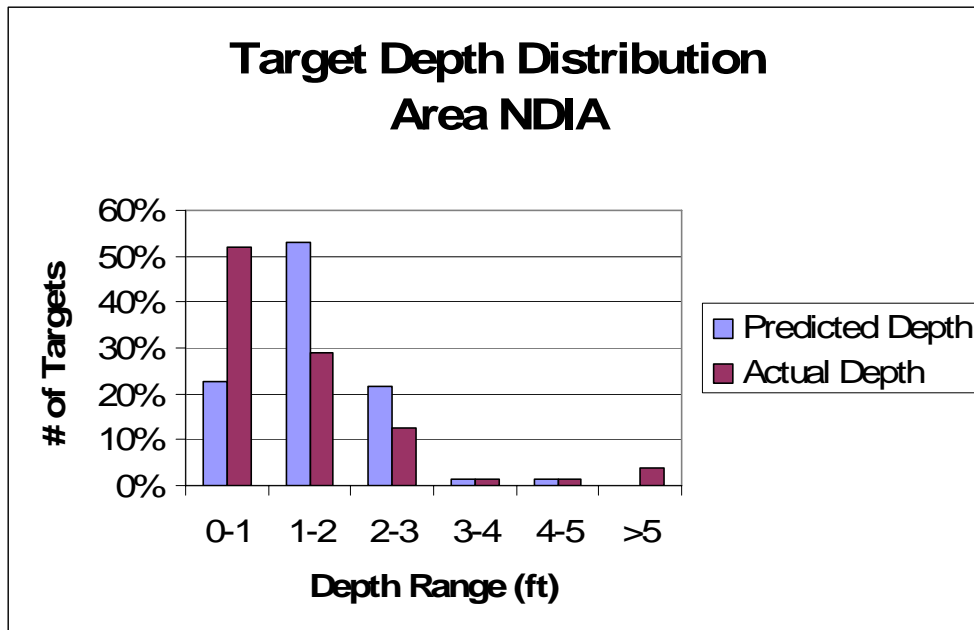
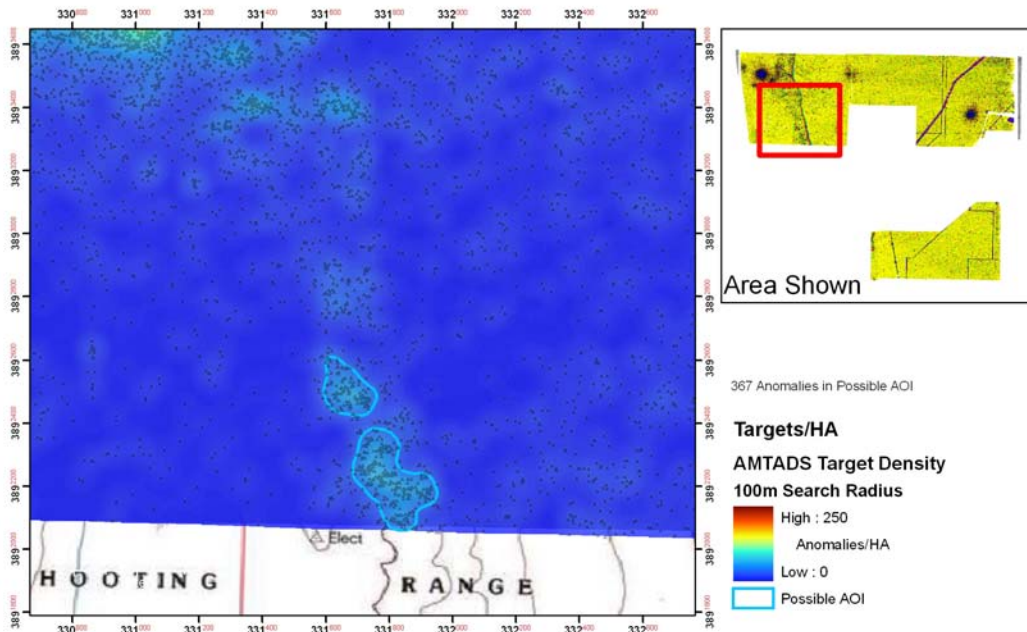


Figure 28. Predicted and observed depths for selected target in the NDIA area.

#### 4.3.5. Possible Areas of Interest

There are a number of areas of interest that have been identified based solely upon the anomaly density analysis results. These areas are outlined in light blue in Figures 29 to 31. Because these areas are associated with a general increase in geologic response this was assumed to be the cause of the elevated anomaly densities and these areas were not evaluated further using advanced analyses or intrusive investigations.



**Figure 29.** Possible areas of interest located in west region of the north study area. These elevated anomaly densities appear to be associated with a region of elevated geologic response.

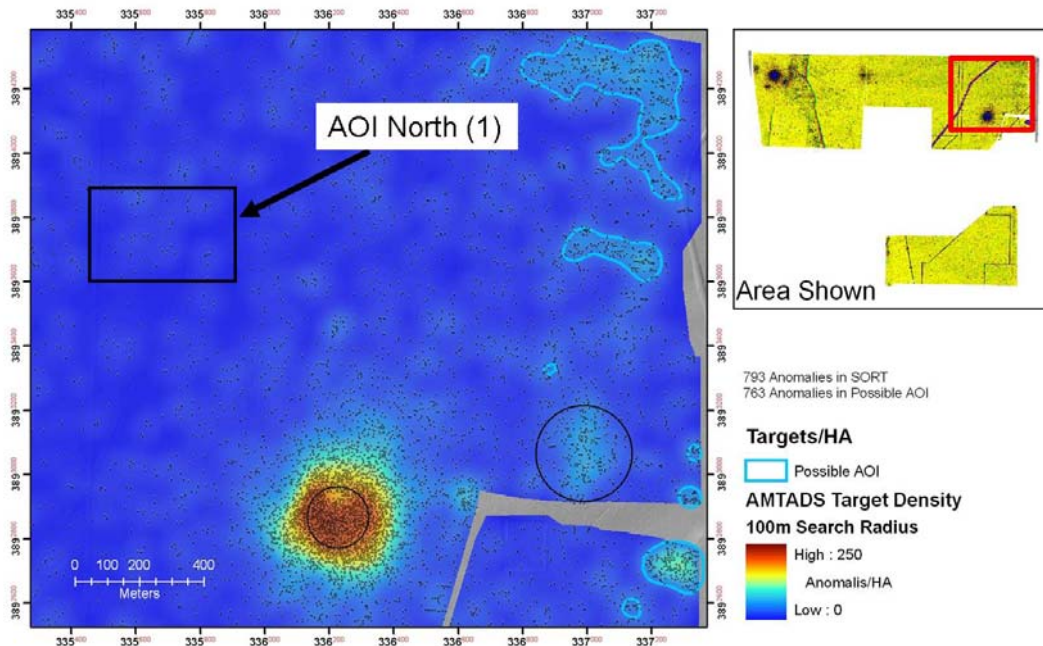


**Figure 30.** Possible areas of interest located in the northern area of the study area. Areas outlined in light blue appear to be associated with regions of elevated geologic response. Additional intrusive investigations were performed in the AOI North area.

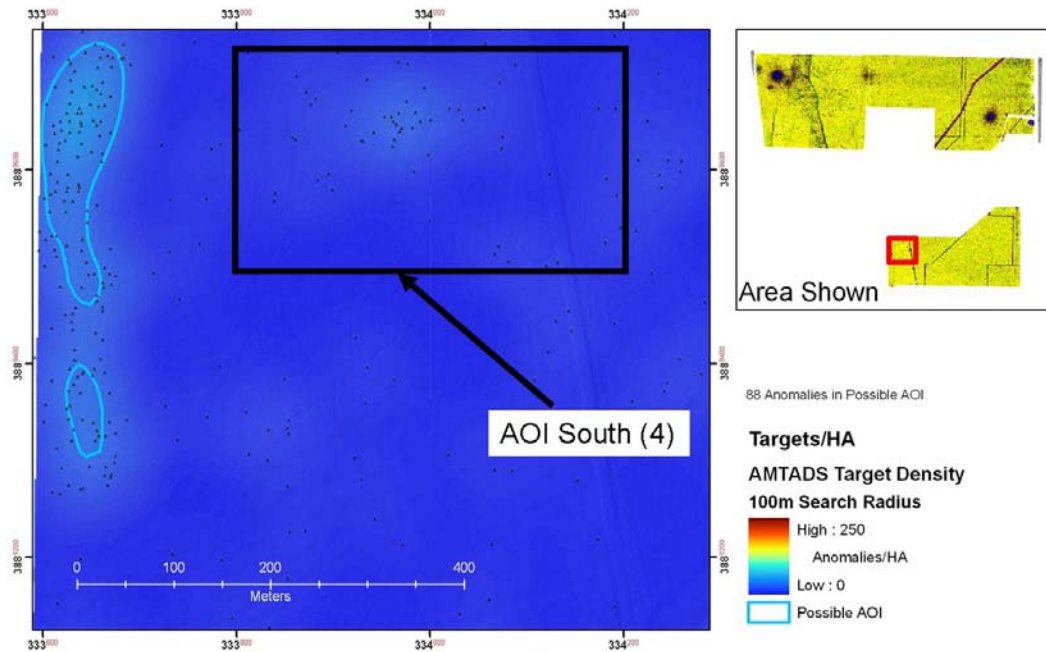


**Figure 31.** Possible area of interest located in NW region of the south study area. Areas outlined in light blue appear to be associated with regions of elevated geologic response. Additional intrusive investigations were performed in the AOI South area.

There were two additional areas that were targeted for further investigation based upon data external to the HeliMag program. The location for the first of these areas AOI-North (also known as AOI-1) is shown in Figure 30. And the second area AOI-South is shown in Figure 31. There is no elevation of anomaly densities for the AOI North area and only a slight elevation in anomaly density for the AOI South area. However the intrusive results (Figure 32) indicate that ordnance related material is present at these sites. Note that the total percentage of targets that were declared ordnance related is significantly less for these areas than the areas where the HeliMag shows high density elevations.

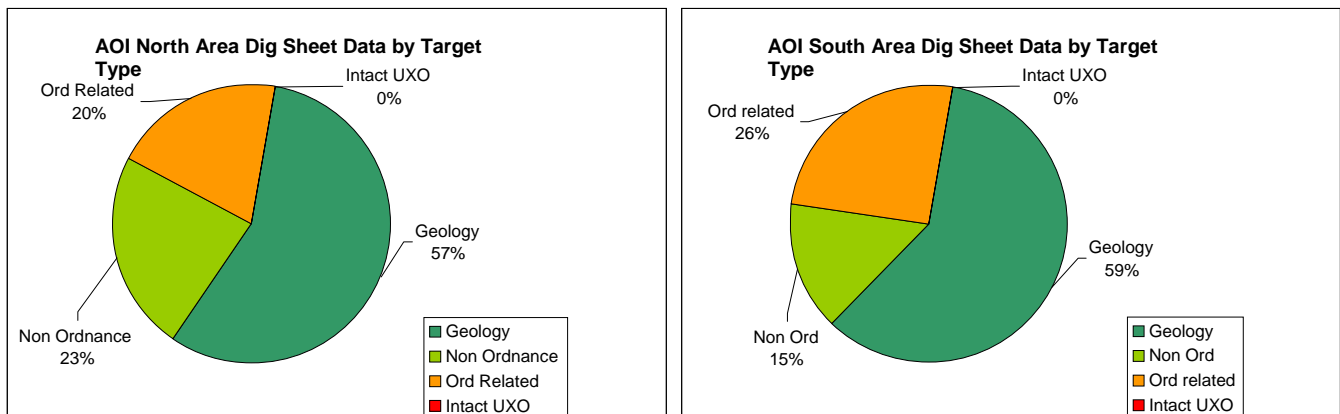


**Figure 32.** Intrusive investigation results for AOI- North and AOI-South.

#### 4.3.6. North-South Linear Corridor Area

In 2007, a north-south linear corridor was surveyed to gain an understanding of the density distribution along this corridor. Aside from the region of high density associated with the SORT area (leftmost panel in Figure 33) we also see moderate anomaly density elevations along the central section.

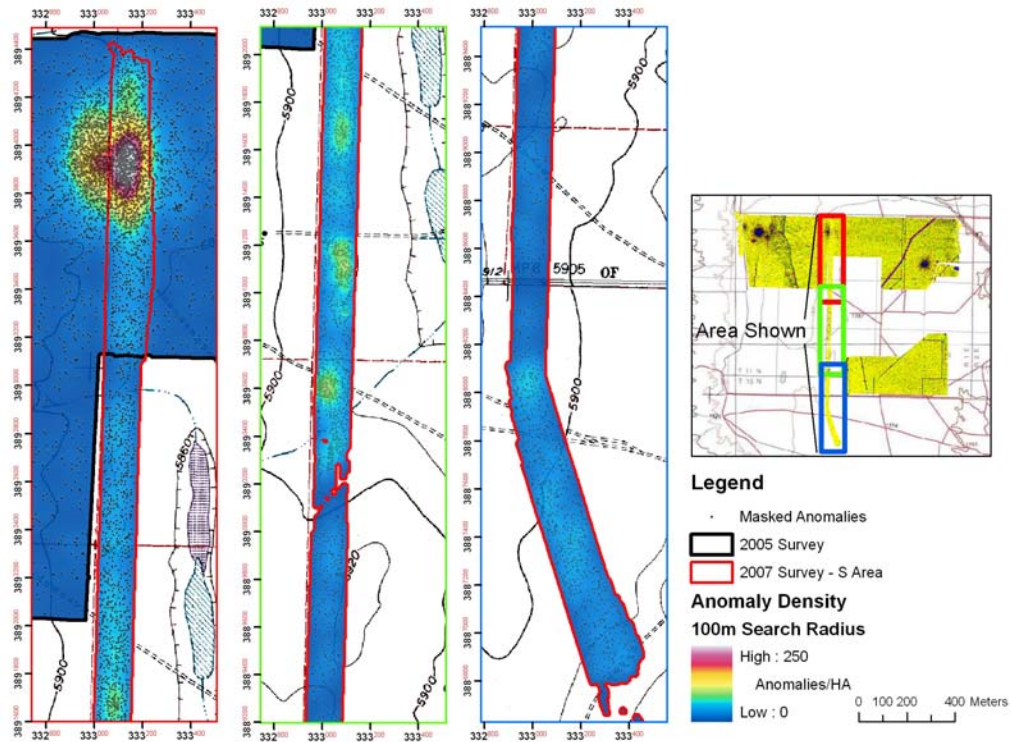


**Figure 33.** HeliMag targets and target density for this north-south corridor area surveyed in 2007.

#### 4.3.7. Northeast Area

An additional area in the NE corner of the survey area was surveyed at the request of USACE. Within the 24.9 acre survey area 685 targets were detected; again, an area with moderately elevated anomaly densities is noted.

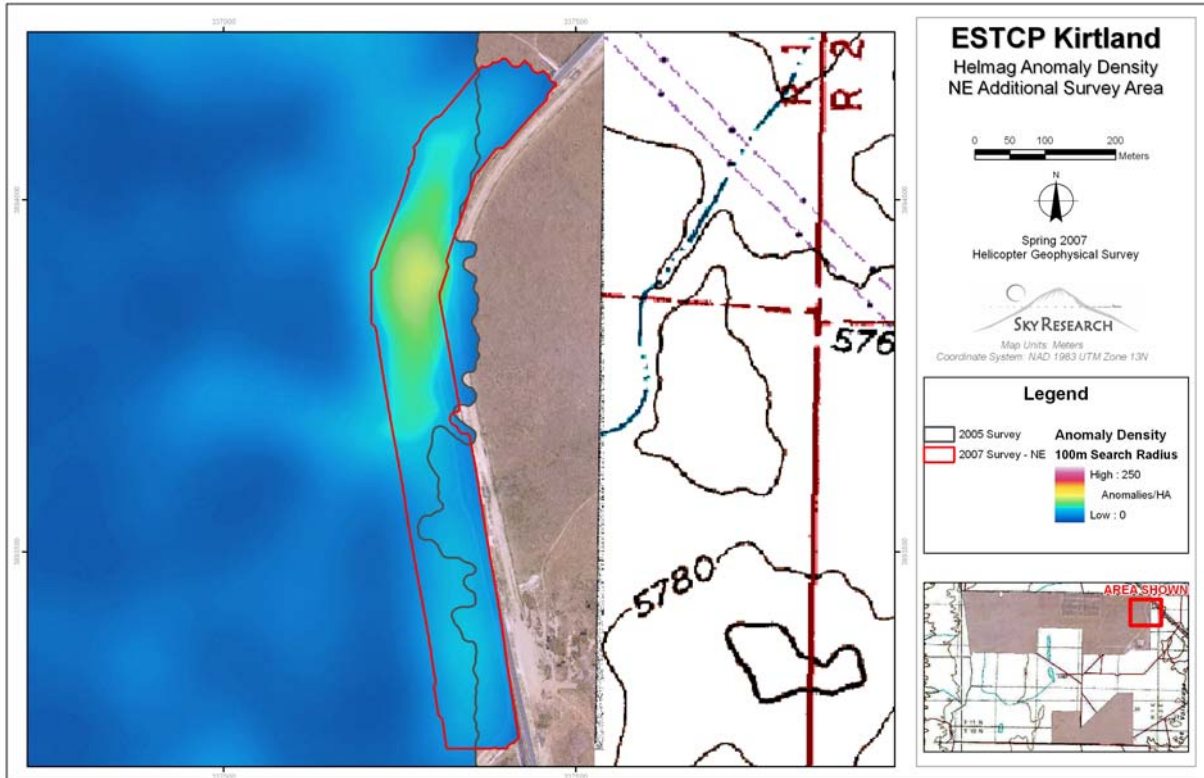


**Figure 34.** HeliMag targets and target density in the additional NE area surveyed in 2007.

#### 4.4. Performance Criteria

The performance of the helicopter magnetometry technology was measured against the criteria listed in Table 8.

**Table 8. Performance Criteria for the Former KPBR HeliMag Technology Demonstration**

<b>Performance Criteria</b>	<b>Description</b>	<b>Type of Performance Objective</b>
Technology Usage	Ease of use and efficiency of operations.	Primary/Qualitative
Geo-reference position accuracy	Comparison of calibration target dipole fit analysis position estimates (in 3 dimensions) to ground truth.	Primary/Quantitative
HeliMag survey area coverage	Actual # acres surveyed/Planned # of survey acres	Secondary/Quantitative
Operating parameters (altitude, speed, overlap, production level)	Field data logs used to calculate the operating parameters.	Secondary/Quantitative
System Noise	Accumulation of noise from sensors and sensor platforms, including GPS, rotor noise, radio frequencies, etc. calculated as the standard deviation of a 20 sec window of processed data collected out of ground effect.	Primary/Quantitative
Data density/point spacing.	(# of sensor readings/sec)/ airspeed	Secondary/Quantitative
MEC parameter estimates	The size and dipole angle estimates of the calibration items are consistent.	Secondary/Quantitative

#### 4.5. Performance Confirmation Methods

Table 9 details the confirmation methods that were used for each criterion, the expected performance, and the performance achieved.

Position accuracy on a dynamic platform is very difficult to measure precisely. We are able to infer the position accuracy of the sensor data by using the position estimates derived from dipole fit analysis of data collected over known targets. Although there are additional error sources (other than just those due to the data positioning) in the dipole fit results, they are almost negligible due to the stability of the magnetometer calibration and the robustness of the dipole fit process. Because reciprocal passes will tend to hide along-track position errors (due to the robustness of the dipole fit process), the dipole fit analyses were performed on each a single pass over the targets.

**Table 9. Performance Metrics Confirmation Methods and Results**

Performance Metric	Confirmation Method	Expected Performance	Performance Achieved
Technology Usage	Field experience using technology during demonstration	Relative ease of use	Pass
Geo-reference position accuracy	Infer sensor position accuracy from position estimates of calibration targets derived using dipole analysis of repeated data collection over calibration targets	Horizontal < 0.25 m Vertical <0.5 m	Horizontal: Mean 0.06 m (SD 0.13 m) Vertical: Mean 0.15 m (SD 0.13 m)
HeliMag survey area coverage	The sum of actual areas surveyed calculated in a geographic information system (GIS) and compared to the final survey area.	95%	99.8% actual areas surveyed (gaps due to obstacle/terrain are excluded from calculations)
Operating parameters (altitude, speed, overlap, production level)	Field data logs used to calculate the operating parameters	Altitude: 1-3 m AGL Speed: 15-20 m/s (30-40 knots) Overlap: 10% Production 300 acres/day	Altitude: Mean 1.6 m (SD .35 m) Speed: Mean 17.8 m/s (SD 2.5 m/s) Overlap: 10% Production:454 acres/day
System Noise	The system noise was calculated as the standard deviation of a 20 sec window of processed high-altitude data.	<1 nT	0.1 to 0.17 nT
Data density/point spacing.	Calculated based upon system sample rate and survey speed (along track) and system geometry and survey line spacing (cross-track track).	0.5 m along-track 1.5 m cross-track	Along-track: Mean 0.178 m (SD .0025 m) Cross-track: 1.5 m
MEC parameter estimates	Comparison of analysis results of repeated data collected over calibration targets.	Size: <.02 m Solid Angle: < 10 °	Size: SD .07 m Solid Angle 6.0 °

## **5. COST ASSESSMENT**

### **5.1. Cost Reporting**

Cost information associated with the demonstration of all airborne technology, as well as associated activities, was tracked and documented before, during, and after the 2005 demonstration to provide a basis for determining the operational costs associated with this technology. Table 10 contains the cost elements that were tracked and documented for the demonstration. The costs associated with the 2007 surveys of additional areas are not included in Table 10, as there were no mobilization and demobilization costs associated with the survey, and to include them in this table would provide an inaccurate estimate of cost per acre.

The costs documented include both operational and capital costs associated with system design and construction; salary and travel costs for support staff; subcontract costs associated with airborne services, support personnel, and leased equipment; and costs associated with the processing, analysis, comparison, and interpretation of airborne results generated by this demonstration. The magnetometers used for the HeliMag technology were provided through a CRADA with NRL; as such, the actual cost of using the technology was not captured in this demonstration. However, we will estimate the true cost of using this technology, in addition to the cost and performance of the technologies demonstrated, in the ESTCP Cost and Performance Report.

### **5.2. Cost Analysis**

The single largest cost element for an airborne survey is the cost of aircraft airtime. In addition, mobilization costs for the helicopter can be significant. Generally, mobilization cost is a function of distance from the home base for the aircraft, equipment, and personnel. Because the helicopter was mobilized a relatively short distance (from Denver to Albuquerque) the costs for mobilization for this demonstration were significantly less than would have been encountered for a demonstration site further away. In addition, the helicopter used for the survey was not demobilized from the site, as the aircraft was sold to another owner immediately following the demonstration. Therefore, the demobilization costs reported are for the demobilization of personnel and equipment only. Data processing and analysis functions made up the bulk of the remaining costs associated with the technical performance of this project.

Project management and reporting were a significant cost for this demonstration, as the project was conducted under the WAA-PP and required more meetings, travel, and reporting than would generally be expected for a production level survey.

Costs associated with validation were not considered in the cost analysis, as the validation was conducted as part of the WAA-PP.

**Table 10. Cost Tracking**

<b>Cost Category</b>	<b>Sub Category</b>	<b>Details</b>	<b>Costs (\$)</b>
Start-up Costs	Pre-Deployment and Planning	Includes planning, contracting, site visit, and site inspection	\$11,197
	Mobilization	Personnel mobilization, equipment mobilization, and transportation	\$17,882
Operating Costs	Helicopter Survey	Data acquisition and associated tasks, including 62 hours of helicopter operation time and 9 hours of standby time	\$242,106
Demobilization	Demobilization	Demobilization, packing, calibration line removal	\$7,022
Data Processing and Analysis	Data Processing	Initial and secondary processing of data	\$18,459
	Data Analysis	Analysis of airborne magnetometry datasets	\$42,880
Management	Management and Reporting	Project related management, reporting and contracting	\$57,507
<b>TOTAL COSTS</b>			
Total Technology Cost			\$397,053.00
Acres Surveyed			5,002
Unit Cost			\$79.38/acre

## **6. IMPLEMENTATION ISSUES**

### **6.1. Regulatory and End-User Issues**

The ESTCP Program Office has established a WAA-PP Advisory Group to facilitate interactions with the regulatory community and potential end-users of this technology. Members of the Advisory Group include representatives of the US EPA, State regulators, Corps of Engineers officials, and representatives from the services. ESTCP staff have worked with the Advisory Group to define goals for the WAA-PP and develop Project Quality Objectives.

There will be a number of issues to be overcome to allow implementation of WAA beyond the pilot program. Most central is the change in mindset that will be required if the goals of WAA extend from delineating target areas to collecting data that are useful in making decisions about areas where there is not indication of munitions use. A main challenge of the WAA-PP is to collect sufficient data and perform sufficient evaluation that the applicability of these technologies to uncontaminated land and their limitations are well understood and documented. Similarly, demonstrating that WAA data can be used to provide information on target areas regarding boundaries, density and types of munitions to be used for prioritization, cost estimation and planning will require that the error and uncertainties in these parameters are well documented in the program.

## **7. REFERENCES**

Blakely, R.J. and R. W. Simpson, 1986, "Approximating edges of source bodies from magnetic or gravity anomalies," *Geophysics*, v.51, p.1494-1498.

Nelson, H., J. McDonald and D. Wright, "Airborne UXO Surveys Using the MTADS," Naval Research Laboratory NRL/MR/6110--05-8874, April 2005.

Tuley, M. and E. Dieguez, "Analysis of Airborne Magnetometer Data from Tests at Isleta Pueblo, New Mexico," IDA Document D-3035, July 2005.

Versar, "Former Kirtland Precision Bombing Range, Conceptual Site Model, V0", 2005.

## 8. POINTS OF CONTACT

**Table 11.** Points of Contact

POINT OF CONTACT	ORGANIZATION NAME ADDRESS	CONTACT INFORMATION	ROLE
Dr. John Foley	Sky Research, Inc. 445 Dead Indian Road Ashland, OR 97520	(Tel) 978.479.9519 (Fax) 720.293.9666	Principal Investigator
Mr. David Wright	Sky Research, Inc. 445 Dead Indian Road Ashland, OR 97520	(Tel) 919.303.3532	Co-Principal Investigator
Mr. Jerry Hodgson	USACE Omaha District 215 N. 17 <sup>th</sup> Street Omaha, NE 68102-4978	(Tel) 402.221.7709 (Fax) 402.221.7838	Federal Advocate
Mr. Hollis (Jay) Bennett	US Army R&D Center (CEERD-EE-C) 3909 Halls Ferry Road Vicksburg, MS 39180-6199	(Tel) 601.634.3924	DoD Service Liaison

**Project Lead Signature:**

